Keio University
1858
CALAMVS
GLADIO
FORTIOR

Shigetora Miyashita

Quantum walk and spacetime structure

Bachelor Thesis

Faculty of Environment and Information Studies
Keio University

Supervision

First Supervisor
Prof. Dr. Rodney Van Meter

February 1, 2023

Abstract

This thesis is concerned with developing and analyzing quantum walk in three different spaces and time structures. We begin with defining the connections between quantum walk and quantum mechanics. While they are known to be equivalent in continuum limits, their relationships in terms of local unitary gates were ambiguous. As a result, each term appears in the Hamiltonian operator, which describes the total energy of a quantum mechanical system and could be seen as an operator of a quantum walk. The results help us to improve our understanding of quantum mechanics from a computer science perspective and vice versa. Furthermore, it also provides a way to deductively derive the quantum walk models from governing equations of quantum mechanics in Sections 3, 4, and 5.

From this perspective, we first provide new quantum walk algorithms for simulating the Schrödinger equation in real space. In the classical literature, numerical schemes for a quantum walk and quantum mechanics are considered different subjects. However, when we implemented both plans using unitary gates, they were found to have the same structure, which made unification possible. As a result, we derived the continuous-time quantum walk from discretizing the time evolution operator of the Schrödinger equation. Furthermore, due to the spectral convergence of the Fourier scheme, the continuous-time quantum walk achieved a faster simulation with exponential precision.

Second, we modify and extend continuous-time quantum walk algorithms to discrete-time ones. The model is derived from the Dirac equation with scalar and vector potential energies. The essential technique employed is the diagonalization of the Dirac matrices, making it possible for quantum computers to access the Dirac spinors in a computational basis. This results in a highly versatile quantum algorithm for simulating the discrete-time quantum walk in (3+1) dimensions. Additionally, we simulated based on the algorithm on IBM Quantum. The result indicated that certain relativistic phenomena are executable on quantum computers.

We finally present a state-of-the-art quantum algorithm for the quantum walk in discrete-spacetime. It is familiar that dynamics of the discrete-time quantum walk propagate in Minkowski spaces. However, the Dirac equation suggests that its dynamics can be considered in curved spacetime. For this reason, we propose an algorithm for the equation by introducing two coins and shift operators. This model demonstrates the first three-dimensional semi-classical gravitational quantum dynamics numerically. Furthermore, we show that the quantum algorithm can simulate relativistic dynamics in black hole backgrounds.

Acknowledgements

I want to thank my supervisor, Professor Rodney Van Meter, who allowed me to work on quantum simulation since I was a freshman. Although he specialized in quantum networking and communications, he always advised me where my research should go.

I also want to thank Dr. Takahiko Satoh, who always gave me grateful opportunities in research activities. His research, publications, and non-research activities could not have been accomplished without him. My thanks also go to Dr. Michihiko Sugawara, who gave me cutting-edge research suggestions even from different schools. I also would like to thank Dr. Michal Hajdušek, who helped me with my research and thesis writing as a mentor, and Dr. Shota Nagayama for hilarious conversations.

The author thanks all the Advancing Quantum Architecture (AQUA) group members for their contributions. My contemporaries, Ryosuke Satoh and Yasuhiro Ohkura, were always my rivals and people to respect at the same time. Furthermore, since I was a sophomore student, Naphan Benchasattabuse has always helped me at work until midnight. Finally, my colleague Nozomi Tanetani and Makoto Nakai largely contributed to the joint work at MITOU Target.

A special thank goes to my friends Katsuhiro and HiraTaku. They were always on my side from the first meeting at a musical club.

Finally, I thank my parents and my twin brother. Throughout my life, they supported me, and I am deeply indebted.

This work was not possible without the support of the MEXT Quantum Leap Flagship Program Grant Number JPMXS0120319794 and the NICT Quantum Camp.

Table of Contents

List of Figures

Chapter 1

Introduction

> *"If, in some cataclysm, all scientific knowledge were to be destroyed, and only one sentence passed on to the next generations of creatures, what statement would contain the most information in the fewest words?" "I believe it is the atomic hypothesis (or the atomic fact, or whatever you wish to call it) that all things are made of atoms, little particles that move around in perpetual motion, attracting each other when they are a little distance apart but repelling upon being squeezed into one another. In that one sentence, you will see enormous information about the world if just a little imagination and thinking are applied."*
>
> — Richard P. Feynman, *The Feynman Lectures on Physics, Volume I*

1.1 Overview

In the last century, theoretical physics progressed remarkably. Two of the most progressive fields were, without a doubt, quantum theory and the theory of relativity [2, 3]. Until now, they have contributed a large amount to the development of modern societies. For example, the theory of relativity is well known as it helped the understanding of our global positions known for GPS (Global Positioning System) through approximation [4]. An example of the applications of quantum theory is quantum technologies [5], which are about to ignite. However, while the two theories seem to be fully established, there is still a gap in practice. The reasons are multiple. However, before explaining its problems, we must precisely distinguish the theories. First, the theory of relativity contains two species: special relativity and general relativity [6]. Second, quantum theory lies under a Planck's constant $h = 6.626 \times 10^{-34}$ J $\cdot$ s while the special relativity is around the speed up light $c = 299,792,458$ m $\cdot$ s^{-1} and the gravitational constant for general relativity is 6.674×10^{-11} m^3 $\cdot$ kg^{-1} $\cdot$ s^{-2}.

Figure 1.1 graphically shows the three physics as a cube. This thesis focuses mainly on quantum theory and special relativity in the horizontal plane.

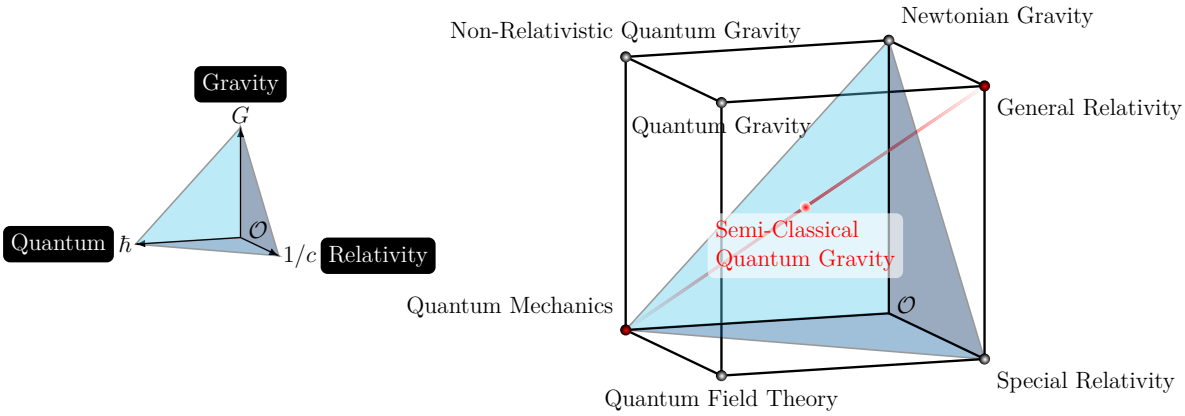

Figure 1.1: The cube of three fundamental theories in physics: quantum, relativity, and gravity. Having the conventional classical mechanics at the origin, each spatial dimension represents a theory. The intersection at the end of three axes are quantum gravity, the ultimate theory. This work focuses on a unified framework for quantum mechanics and general relativity known as semiclassical quantum gravity.

Furthermore, I must note that there are two systems in the present investigation: the control system and the target system. In a typical quantum simulation, we use a quantum system as a controlling system to understand another system as a target system. For the target system, this thesis mainly focuses on the interdisciplinary field of quantum mechanics and general relativity, i.e., semiclassical quantum gravity.

1.2 The problem

In this section, I will explain the generic problems that arise in understanding two theories: the quantum theory and the theory of relativity. Even with all the science available, (1) experimental science, (2) theoretical science, (3) computational science — quantum theory is difficult to acknowledge fully. In the latter, I will explain why understanding the theories is difficult with each approach.

First, any experiment is limited only to test systems that are accessible. The fundamental approach in experimental science is mathematical induction, which means we logically obtain conclusions from the inference via observing exceptional cases to get data. In history, this approach is the first scientific method, and all other forms must rely on the laws obtained through experiments. This method, however, faces difficulties when the required resource for setting up an investigation surpasses the available (affordable) help. A simple example was gravitational wave detection. Although there were indirect observations that accented the evidence of the existence of gravitational waves, direct

observation has been difficult because of the cost required for setting experiments on such large-scale and long-distant objects. Similarly, experiments become expensive when imposed on small-scale entities, such as atoms and quanta.

Second, (narrowly defined) theoretical approaches are limited to analyzing analytically solvable systems. This approach is known as the second scientific method. In theoretical sciences, we derive general laws based on particular rules or mathematical fundamentals such as axioms. It faces difficulties when the calculations are difficult to solve analytically. For example, we generally want to represent a solution with rational numbers or a combination of transcendental numbers and elementary functions. On the other hand, it is not always possible to solve complex equations such as partial differential equations. For instance, the Schrödinger equation, a fundamental equation in quantum mechanics, is known to be unsolvable when the potential energy cannot be reduced to a simple form. For that purpose, perturbation methods are widely used to have an approximated solution. However, perturbation methods also face difficulties for many-body quantum systems, so it is more desirable to analyze strategies computationally for such systems.

Third, (classical) computational science also has limitations in analyzing systems that require beyond computational power, i.e., memory size or time. In computation, we usually use numerical approximation to derive the solution with a certain precision inductively. In this approach, there are difficulties similar to those of the theoretical approaches, but with reasons. That is, a solution cannot be obtained with fair precision if the problem contains too large a degree of freedom (such as many-body systems). This happens because memory size and time are required in proportion to the degree of freedom in most cases. We want exascale computers to compute large and dynamic systems for many-body problems.

1.3 Quantum walk

For the problems mentioned earlier, a new computational paradigm, a quantum computer, was conceived [7]. Quantum computers were initially inspired by mimicking nature exactly with a computer [8]. The notion has been formulated as an analog quantum simulator, and a logical, universal quantum automaton has been introduced as a quantum computer [9]. The past decade has seen the rapid development of quantum algorithms with potential application to the so-called quantum simulation [10, 11].

Quantum walk is one of the prominent quantum algorithms defined by analogy to the classical random walk [12]. Until now, two kinds of quantum walks, continuous- and discrete-time quantum walks, have mainly been investigated [13]. Due to their definition, a continuous-time (and discrete-space) quantum walk can be considered a single-particle quantum mechanical dynamics governed by the time-dependent Schrödinger equation [14].

In contrast, a discrete-time (and discrete-space) quantum walk can be considered a time-dependent Dirac equation, which arises in the unique relativistic quantum mechanics [15].

1.4 Spacetime structure

Recently, a new family of quantum walks has gained the attention of the masses. Although the literature is scarce, specific parameterized walk in that model is known to converge into a Dirac equation in curved spacetime [16, 17].

1.5 Summary of results

In this thesis, I present quantum algorithms to simulate the three kinds of quantum dynamics, which are exponentially precise with an improvement in the quantum gate count. Furthermore, I compare and contrast the structure of quantum algorithms towards simulating quantum field theories by quantum walks and their extension, known as a quantum cellular automaton.

In Chapter 2 quantum walk is briefly reviewed. We begin with introducing the concept of quantum information in order to provide concrete understanding of quantum walk algorithms in the latrer sections. Chapter 3 is devoted to explain the implementation of continuous-time quantum walk. The ordinary continuous-time quantum walk is defined as the discrete analog of the time-dependent Schrödinger equation for a free particle [18]. We utilize the fact to identifying the quantum walk operators including the case that potential energy exists. Quantum walk turns into discrete-time model in Chapter 4. By introducing the quantum coin with auxiliary qubits, the evolution operator becomes non-commutative which gives the time discrete. In this case, the quantum walk can be interpret as the time-dependent Dirac equation [15]. We rederive the quantum walk from the equation including scalar and vector potentials. In Chapter 5, we extend the aforementioned walk to arbitrary spacetime. The key idea is to introduce extra coin operators to include the semi-classical gravitational effects. We finally summarize all the work in the concluding Chapter 6.

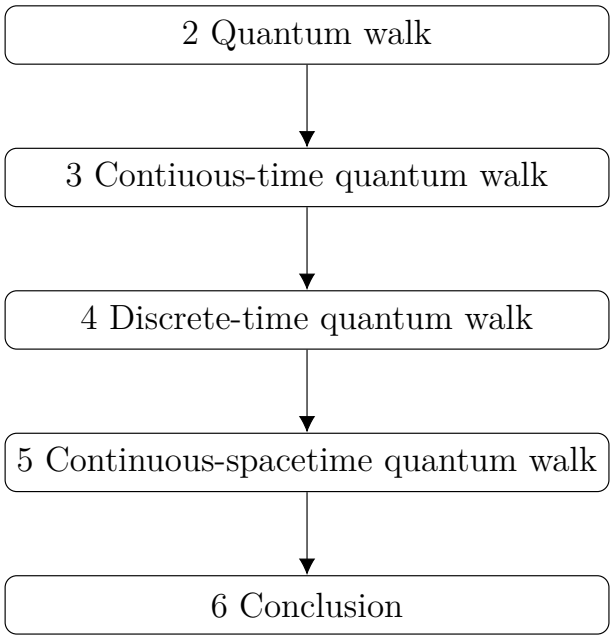

Figure 1.2: The flow diagram of topics presented in this thesis. Each topic relies on the foundation of the previous chapters.

Chapter 2

Quantum walk

This chapter reviews the basics of relativistic and non-relativistic quantum information. Ordinary non-relativistic quantum information yields substantial advantages in computation, communication, and so on. For example, the minimum element to describe the quantum mechanics of qubits is composed of the qubits and quantum states given in Sec. 2.1.1, quantum measurement in Sec. 2.1.2, quantum operation in Sec. 2.1.3.

2.1 Overview

2.1.1 Qubits and quantum states

It is well known that the fundamental unit of quantum information is a qubit. In pure states, a qubit is represented as a column vector.

$$\begin{pmatrix} \alpha \\ \beta \end{pmatrix}, \tag{2.1.1}$$

where $\alpha, \beta \in \mathbb{C}$ are complex numbers that are the unit norm $|\alpha|^2 + |\beta|^2 = 1$. The Hilbert space is the two-dimensional vector space $\mathcal{H}$ that is complete and can define the inner products. The complex column vector that represents the pure states of qubits

$$\begin{pmatrix} \alpha \\ \beta \end{pmatrix} = \alpha \begin{pmatrix} 1 \\ 0 \end{pmatrix} + \beta \begin{pmatrix} 0 \\ 1 \end{pmatrix}, \tag{2.1.2}$$

is called the state vector. Let $\alpha = \cos\theta/2$ and $\beta = e^{i\phi}\sin\theta/2$, unity of the norm will always be conserved.

$$\left\| \begin{pmatrix} \cos\theta/2 \\ e^{i\phi}\sin\theta/2 \end{pmatrix} \right\|_2 = 1. \tag{2.1.3}$$

Here, we define the ket vectors for the convention of writing complex column vectors:

$$\begin{aligned} |0\rangle &\doteq \begin{pmatrix} 1 \\ 0 \end{pmatrix}, \\ |1\rangle &\doteq \begin{pmatrix} 0 \\ 1 \end{pmatrix}, \\ \Rightarrow \begin{pmatrix} \cos\theta/2 \\ e^{i\phi}\sin\theta/2 \end{pmatrix} &\doteq \cos\frac{\theta}{2}|0\rangle + e^{i\phi}\sin\frac{\theta}{2}|1\rangle \coloneqq |\psi\rangle\,, \end{aligned} \tag{2.1.4}$$

where we note the set of complete orthogonal vectors $\{|0\rangle, |1\rangle\}$ are known as the computational basis. The ket vector defined in Eq. (2.1.4) can visually be represented using the Bloch sphere shown as Eq. (2.1). The graphical representation would indicate the

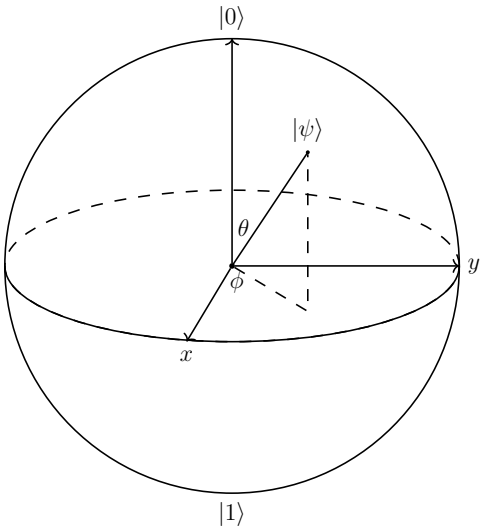

Figure 2.1: The Bloch sphere representation of a qubit.

computational power based on qubits compared to classical bits, as the latter can only take precisely two values. At the same time, the former can be superposed of $|0\rangle$ and $|1\rangle$. Straightforwardly, the degree of freedom exponentially increases as the number of qubits increase. On the contrary, some theorems physically prohibit every operation from being efficiently performed with qubits, and they are called no-go theorems.

2.1.2 Quantum measurement

There are several measurements of qubits, but the most simple is a projective measurement. We select a base of qubits to measure.

$$\begin{aligned} &|\phi\rangle\,, \\ &|\phi^{\perp}\rangle\,. \end{aligned} \tag{2.1.5}$$

and apply the projector

$$\begin{aligned} \Pi_0 &= |\phi\rangle\langle\phi|\,, \\ \Pi_1 &= |\phi^\perp\rangle\langle\phi^\perp|\,. \end{aligned} \tag{2.1.6}$$

We finally obtain the classical output $\{0, 1\}$. Note that we can write the projection with inner products.

$$\begin{aligned} p_0 &= \mathrm{Tr}\{\Pi_0 |\psi\rangle\langle\psi|\} = |\langle\phi|\psi\rangle|^2, \\ p_1 &= \mathrm{Tr}\{\Pi_1 |\psi\rangle\langle\psi|\} = \left|\langle\phi^\perp|\psi\rangle\right|^2. \end{aligned} \tag{2.1.7}$$

2.1.3 Quantum operation

On classical computers, the operation is always deterministic

$$f(\{0,1\}^*) = \{0,1\}^*, \tag{2.1.8}$$

where f acts on a binary to output a different binary. This equation is also valid on quantum computers.

$$f(|\psi_{\mathrm{in}}\rangle) = f(|\psi_{\mathrm{out}}\rangle). \tag{2.1.9}$$

However, quantum computers do not give the quantum states deterministically but probabilistically by quantum measurements described in the last section. However, there is a deterministic formulation known as a completely-positive trace preserving (CPTP) map. In a single qubit case, a 2-vector is mapped to an output vector with the same shape

$$U|\psi_{\mathrm{in}}\rangle \doteq \begin{pmatrix} a & \sqrt{1-a^2} \\ \sqrt{1-a^2} & -a \end{pmatrix} \begin{pmatrix} \alpha \\ \beta \end{pmatrix} = \begin{pmatrix} a\alpha + \sqrt{1-a^2}\beta \\ \sqrt{1-a^2}\alpha - \beta a \end{pmatrix} \doteq |\psi_{\mathrm{out}}\rangle\,. \tag{2.1.10}$$

2.2 Simulating quantum dynamics

Simulating quantum dynamics classically is a complex problem in terms of computational complexity. For instance, due to the exponential growth of the Hilbert space concerning the number of particles and spacetime points, the space complexity is generally given as 2^n where n is the number of qubits. Furthermore, the time complexity is also offered as an exponential function.

On the other hand, quantum computers can handle the Hilbert space with a linear scaling number of qubits. This is because their computation is based on "qubits," meaning that the Hilbert space of the simulator also grows exponentially (2^n). The following briefly summarizes three fundamental quantum mechanical equations for quantum simulations.

2.3 Continuous-time quantum walk

The most basic equation of quantum mechanics is the Schrödinger equation.

$$i\frac{\partial}{\partial t}\psi = \left[-\frac{1}{2}\nabla^2 + V\right]\psi. \tag{2.3.1}$$

The symbol ψ in the above partial differential equation denotes the state vector of a particle, ∇ is a differential operator, and V is a position-dependent potential function. Without the imaginary unit i, the equation can be reduced to a diffusion equation. However, due to the fictional contribution, the differential equation becomes hermitian.

In a discrete space, it is known that the time-dependent Schrödinger equation for a free particle turns into a continuous-time quantum walk [14]. The Hamiltonian can be considered the operator of a continuous-time quantum walk. Specifically, the kinetic energy operator in the Schrödinger can be regarded as the Laplacian matrix in the continuous-time quantum walk.

2.4 Discrete-time quantum walk

Another fundamental equation is the Dirac equation which describes the dynamics of relativistic particles.

$$i\frac{\partial}{\partial t}\psi = \left[\boldsymbol{\alpha}\cdot(-i\nabla + e\boldsymbol{A}) + \beta m - e\phi\right]\psi. \tag{2.4.1}$$

Dirac matrices $\boldsymbol{\alpha}, \beta$ are introduced to represent the square root of the differential operator in the Schrödinger equation. In this regime, they move at around the speed of light. One of the remarkable properties of this equation is the linear dispersion when the mass is negligible. The Dirac equation can be modified further to the Weyl and Majorana equations corresponding to each name of the fermions.

With discrete space and time, it is known that the time-dependent Dirac equation becomes a discrete-time quantum walk [15].

2.5 Discrete-spacetime quantum walk

When the Dirac equation is coupled to gravity, it turns to the partial differential equation of the following form.

$$i\frac{\partial}{\partial t}\psi = \left[-i(g^{00})^{-1}\gamma^0\gamma^i(\partial_i + \Omega_i - ieA_i) + (g^{00})^{-1}\gamma^0 m - (i\Omega_0 + eA_0)\right]\psi. \tag{2.5.1}$$

This equation introduces γ matrices to describe the particle dynamics in spacetime.

The time-dependent Dirac equation in curved spacetime can also be formulated as quantum walks with specific parameters, discrete space, and time [16, 17]. We call this model as the discrete-spacetime quantum walk and will discuss about this walk in Sec. 5.

Chapter 3

Continuous-time quantum walk

This chapter proposes an efficient quantum spectral method for simulating the continuous-time quantum walk. The implementation of the quantum circuits for the continuous-time quantum walk has not been paid much attention due to the unclear structure of algorithms. In this work, we utilize the fact the continuous-time quantum walk is a continuous-time discrete-space model of the free Schroödinger equation. By evaluating the kinetic energy operator of the Schrödinger equation in the Fourier space, we show that the continuous-time quantum walk can be reduced to a straightforward form with exponential convergence. This indicates that the digital quantum simulation of the single-particle Schrödinger equation is now tractable on quantum computers.

3.1 Overview

The primary application of quantum computers is digital quantum simulation [19]. After Feynman's proposal of quantum automata [8], dozens of quantum algorithms are developed in quantum information science [20–23]. One of the attractive algorithms is the quantum walk [24]. It can be thought of as the quantum analog of the classical random walk and the discrete analog of the quantum mechanics, i.e., a continuous-time quantum walk can be regarded as the dynamics of the single-particle time-dependent Schrödinger equation [18].

Both classical and quantum computers have investigated continuous-time quantum walks. However, one time-dependent Schrödinger equation has primarily been implemented with Fourier spectral methods on classical computers [25–28]. The partial differential equation becomes an ordinary form in the Fourier domains. Furthermore, owing to the approximation by trigonometric polynomials, the resulting scheme has exponential convergence concerning the special resolution n.

However, work on implementing continuous-time quantum walks on computers is scarce. This is probably due to the connection between continuous-time quantum walk and the time-dependent Schrödinger equation is not widely investigated in quantum information science.

This chapter introduces the continuum Hamiltonian of quantum mechanics and derives the efficient quantum spectral methods for a continuous-time quantum walk. This deductive work provides an advantage in computational complexities. For the space, the complexity is given by n with the n grid points, unlike that of classical methods. Moreover, the time complexity is provided as a polynomial to n.

3.2 The continuum Hamiltonian

We start with defining the non-relativistic input Hamiltonian. The Hamiltonian obeys the Schrödinger equation is written as

$$H = -\frac{1}{2}\nabla^2 + V. \tag{3.2.1}$$

The continuous-time quantum walk is known to converge the Schrödinger equation in the continuum limits.

3.2.1 Time-discretization

We discretize the equation in terms of time to derive the quantum spectral methods for the time-dependent Schrödinger equation. Namely, we use the product formula (operator splitting) for the time discretization to express the corresponding time evolution operator based on non-commuting Hamiltonians with local Hamiltonians. This procedure is identical to the one found in classical Fourier pseudospectral methods [29–35]. Our goal is to find the wave function that has evolved t.

$$|\psi(t)\rangle = \mathcal{T}\left[e^{-i\int_0^t H(s)ds}\right]|\psi(0)\rangle\,. \tag{3.2.2}$$

$\mathcal{T}$ holds the time-ordering of the exponential operators. Now, we think of the explicit discretization of time of the exponentials. In discretization, we approximate the continuous time by the discrete time. In other words, we rewrite the unitary operators as products (that is, the operator splitting) [36–39]. In general, splitting errors arise from the non-commuting terms, but the formula for the $2k$th-order product formula is written by [40]

$$\begin{aligned} \mathscr{S}_2(t) &:= e^{-i\frac{t}{2}\mathbf{A}} \cdot e^{-it\mathbf{B}} \cdot e^{-i\frac{t}{2}\mathbf{A}}, \\ \mathscr{S}_{2k}(t) &:= \mathscr{S}_{2k-2}(u_k t)^2 \mathscr{S}_{2k-2}((1-4u_k)t)\mathscr{S}_{2k-2}(u_k t)^2. \end{aligned} \tag{3.2.3}$$

The product of the exponential operators allows us to treat the total time evolution operators with local unitaries, with discrete time as the sum of small time steps. As a result, the original Schrödinger Hamiltonian is decomposed into the following form.

$$\begin{aligned} H_1 &= -\frac{1}{2}\nabla^2, \\ H_2 &= V. \end{aligned} \tag{3.2.4}$$

Then the time evolution operator for each term can be written as

$$\begin{aligned} \mathscr{S}_2(t) =& e^{-i\frac{t}{2}H_1} \cdot e^{-itH_2} \cdot e^{-i\frac{t}{2}H_1}, \\ \mathscr{S}_{2k}(t) =& \mathscr{S}_{2k-2}(u_k t)^2 \mathscr{S}_{2k-2}((1-4u_k)t)\mathscr{S}_{2k-2}(u_k t)^2. \end{aligned} \tag{3.2.5}$$

As mentioned, the 2nd-order Suzuki-Trotter decomposition guarantees up to 2nd-order in time.

$$\begin{aligned} \left\| \mathscr{S}_2(t) - e^{-itH} \right\| \leqslant & \frac{t^3}{12} \sum_{\gamma_1=1}^{\Gamma} \left\| \left[\sum_{\gamma_3=\gamma_1+1}^{\Gamma} H_{\gamma_3}, \left[\sum_{\gamma_2=\gamma_1+1}^{\Gamma} H_{\gamma_2}, H_{\gamma_1} \right] \right] \right\| \\ & + \frac{t^3}{24} \sum_{\gamma_1=1}^{\Gamma} \left\| \left[H_{\gamma_1}, \left[H_{\gamma_1}, \sum_{\gamma_2=\gamma_1+1}^{\Gamma} H_{\gamma_2} \right] \right] \right\|. \end{aligned} \tag{3.2.6}$$

The details on Trotter errors are elaborated in Ref. [40].

3.2.2 Space-discretization

Next, we consider the spatial discretization of the time-dependent Schrödinger equation [39, 41]. We need to specify the basis function to derive the quantum spectral methods. While the quantum algorithm for the Chebyshev pseudospectral method is proposed, we have chosen the Fourier basis for convenience and cogency in treating quantum systems. Similarly to time discretization, we take the original continuous domain as the discrete domain with a truncated computational cell volume Ω with n grids. Subsequently, we define the pair:

$$\begin{aligned} r_p &= \frac{p\Omega}{n} && p \in G, \\ k_p &= \frac{2\pi p}{\Omega} && p \in G, \\ G &= \left[-\frac{n-1}{2}, \frac{n-1}{2} \right] && \subset \mathbb{Z}^3. \end{aligned} \tag{3.2.7}$$

Here, r_p is a reciprocal lattice vector at p, and k_p corresponds to the vector in the Fourier space. We note that in Fourier space, the solution is approximated as a linear combination of the trial functions on a Fourier basis. This is the gist of the spectral method, and we will have the spectral (exponential) convergence and accuracy for smooth solutions.

$$\|\psi_h - \psi\| \leqslant n^{s-r} \|\psi\|_{H^s} \quad \text{for } s > r > d/2 \in \mathbb{R}. \tag{3.2.8}$$

3.3 Continuous-time quantum walk

In this section, we elucidate the explicit quantum circuit of quantum spectral methods for the continuous-time quantum walk. The scheme is based on Fourier spectral methods but with the quantum speed up via the quantum Fourier transforms and diagonal unitaries. In its implementation, we show the construction of optimal quantum circuits for a single-trotter step. The trotter terms include the kinetic energy $e^{it\frac{1}{2}\nabla^2}$, potential energy e^{-itV} as stated in Sec. 3.2.

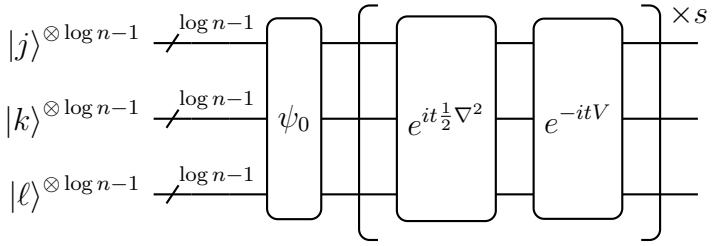

Figure 3.1: Schematic of the quantum spectral method for continuous-time quantum walks. The first block is the initial state preparation block and the next repeating s blocks are the time-splitting operators.

Theorem 3.3.1. *Consider the continuous-time quantum walk on a cycle with the Hamiltonian as defined in (3.2.4). Then for any $t \in \mathbb{R}$ (propagation time) and ϵ (error reliance) there exists a unitary operation e^{-itH} which can be implemented on quantum computers with complexity*

$$O(\text{poly}(\log(1/\epsilon))). \tag{3.3.1}$$

We begin with defining the quantum registers. Since the spinor of the Schrödinger equation in 3 dimensions, $\psi \in L^2(\mathbb{R}^3) \otimes \mathbb{C}$, has n grid points, the number of qubits is given by $3n$. To map the spinor onto qubits using the real space grid representation, we use $\mathscr{Q}_1 - \mathscr{P}_0$ elements where each cell volume is equal. Projecting the spinor onto the qubits, we get the discretized wave function ψ_n as summations expressed as

$$\psi_n = \sum_{j=1}^{n} \sum_{k=1}^{n} \sum_{l=1}^{n} \alpha_{j,k,l} \left|j\right\rangle \left|k\right\rangle \left|\ell\right\rangle, \tag{3.3.2}$$

where each ket vector has 2^n probability amplitudes.

We elucidate the quantum circuit implementation based on quantum spectral methods in the next procedure. The Schrödinger Hamiltonian 3.2.4 has a second-order spatial derivative, which cannot be easily implemented in the computational basis due to non-diagonal elements. In the latter, we show its implementation with local unitaries.

3.3.1 Implementing the kinetic energy term

Lemma 3.3.2. *For any $t \in \mathbb{R}$ operation $e^{it\frac{1}{2}\nabla^2}$ can be performed with gate complexity $O(\log n \log\log n)$.*

Proof. Consider the kinetic energy term $e^{it\frac{1}{2}\nabla^2}$ of the Schrödinger equation. The term can be evaluated in the Fourier space.

$$e^{it\frac{1}{2}\nabla^2} = \mathrm{QFT} e^{-it\frac{1}{2}\mathbf{p^2}} \mathrm{QFT}^\dagger \tag{3.3.3}$$

Furthermore, the spatial dimensions can be written as the tensor product of each dimension.

$$e^{-it\frac{1}{2}\mathbf{p^2}} = e^{-it\frac{1}{2}\mathrm{p}^2} \otimes e^{-it\frac{1}{2}\mathrm{p}^2} \otimes e^{-it\frac{1}{2}\mathrm{p}^2} \tag{3.3.4}$$

Since the momentum operator in each direction can be regarded as a function, we can

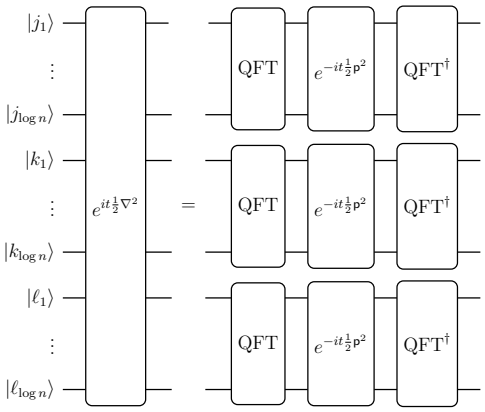

Figure 3.2: Depiction of the quantum circuit for the decomposition of the kinetic energy term into QFT and diagonal operators.

rewrite it in the Z basis,

$$\frac{1}{2}p = -\frac{\pi}{\Omega}\sum_{j=1}^{\log n} 2^j Z_j, \tag{3.3.5}$$

where Ω denotes the spatial volume. By facilitating two Z bases, we can obtain the momentum function.

$$\frac{1}{2}p^2 = \frac{\pi}{\Omega}\left(\frac{1}{3}(n^2-1) + \sum_{j=1}^{\log n-1}\sum_{k\geqslant j}^{\log n} 2^{j+k+1} Z_j Z_k\right). \tag{3.3.6}$$

We finally get the ordinary momentum operator by exponentiating the function. □

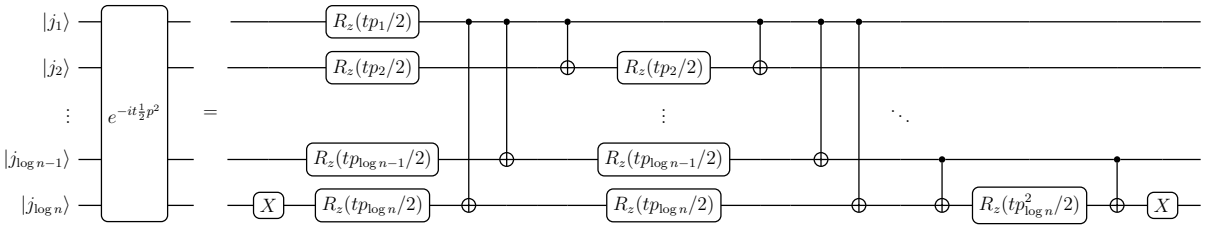

Figure 3.3: Depiction of the quantum circuit for the decomposition of the shifted quadratic momentum operator into elementary gates.

3.3.2 Implementing the potential energy term

Lemma 3.3.3. *The quantum circuit e^{-itV} with error tolerance ϵ can be performed with gate complexity $O(\text{poly}(\log(1/\epsilon)))$.*

Proof. Consider the potential energy term e^{-itV} of the time-dependent Schrödinger equation. It can be decomposed into a one-dimensional system in the same way as the kinetic energy term. To construct a 1-dimensional function, we entail the work by [1]. Their work implements a process in the Z basis with Walsh transformed function. □

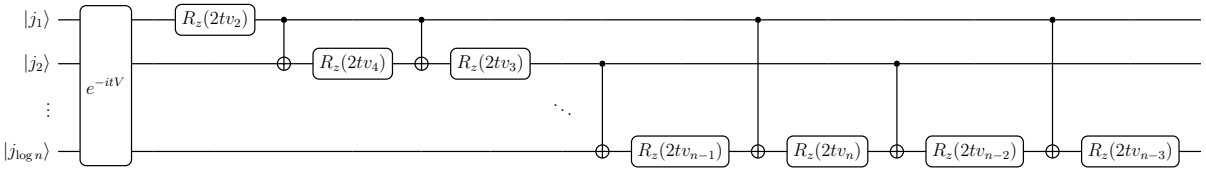

Figure 3.4: Depiction of the quantum circuit for the decomposition of the potential energy term into elementary gates via Walsh transformed function [1].

3.4 Simulation results

The primary research question was to investigate the polynomial-time quantum algorithm for the time-dependent Schrödinger equation in $1+1$ dimensions. Through several examples, we attempted to verify and test how straightforward and efficient the algorithm is. On top of IBM's open-source SDK Qiskit, we examined the quantum simulation classically. To have the fine mesh to evaluate the behavior of the simulation, we have chosen to use a total of 11 qubits (1 qubit for the spinor $|s\rangle$ and ten qubits for the space representation $|j\rangle$) with 512 grids. Using the result, we compare it to the classical pseudospectral algorithm with the same settings. Furthermore, we have implemented the quantum algorithm on an actual device and performed a digital quantum simulation with a 4-qubit system.

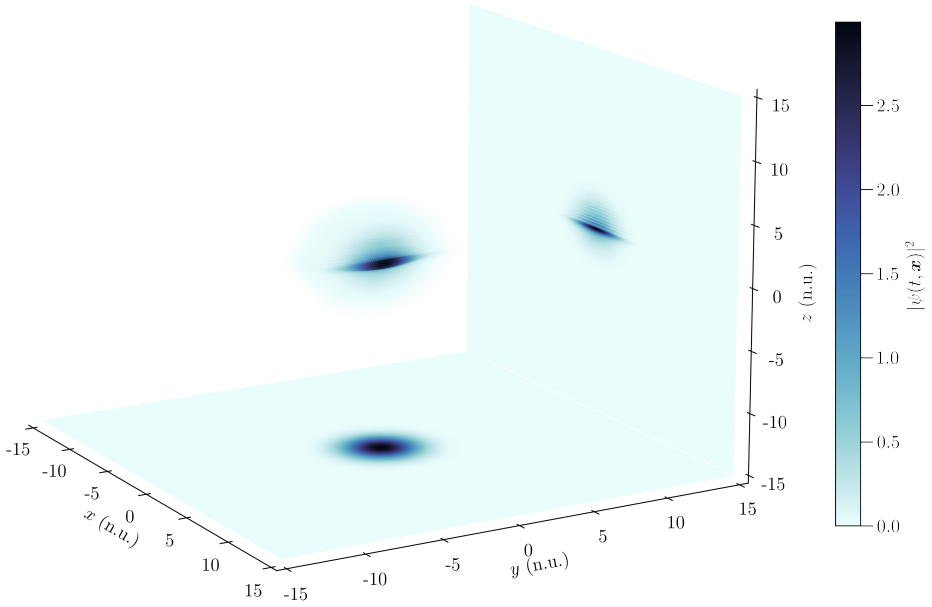

Figure 3.5: Three-dimensional simulation of the quantum tunneling through the Eckart barrier. Each axis represents the space in Cartesian coordinates. At $t = 0$, initial wave packets is centered around $x = 0, y = 0, z = 9$. The plot shows the packet hit the potential barrier $z = 0$ at $t = 0.6$ with transmission.

Fig. 3.5 shows the simulation results of the quantum tunneling through the Eckart barrier in three dimensions. The simulation was executed on Qiskit's statevector simulator. At $t = 0$ initial wave packet is set at around $z = 5$. As time goes on, it evolves toward the Eckart barrier allocated in the center $z = 0$. The figure shows a specific weight of the wave packet tunneling through the barrier, and others are reflected and show the fringe. This is one of the quantum-specific effects which does not occur in classical scattering problems.

We finally show the spectral convergence in Fig. 3.6. Our quantum (Fourier) spectral method is compared with the 2nd-order finite difference method. The plot clearly shows the spectral methods' exponential convergence from $n = 4$ to $n = 32$.

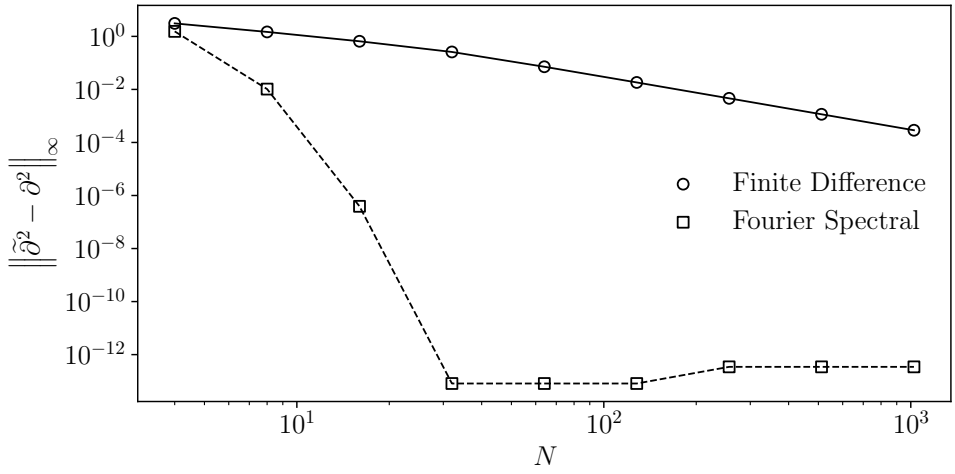

Figure 3.6: log-scale plot of the error estimation of the 2nd-order differential operator. The horizontal axis shows the number of grid points in a single dimension while the vertical axis show the convergence rate. The plot shows spectral convergence.

3.5 Conclusions & discussion

This chapter showed the efficient quantum spectral methods for a continuous-time quantum walk. In addition, we performed the classically emulated digital quantum simulation using Qiskit. In the simulation, we utilized 24 qubits, which is currently not feasible on noisy intermediate-scale quantum (NISQ) devices. But using classical, alternative direction iteration (ADI) methods, we can simulate the three-dimensional quantum walk with iterative one-dimensional quantum walks. Furthermore, we can see many exciting problems in 1 dimensional systems with a small number of qubits.

This work can be extended in several directions. First, one should consider introducing the non-commutativity, i.e., the discrete-time quantum walk. The implementation is a little more complex in the walk as additional degrees of freedom are known as the spin. The spiral system is now described by the Dirac equation with the two by 2 Dirac matrices to introduce the spin. The quantum spectral methods are expected to be technically challenging, especially in multi-dimensions.

The second direction is to extend the computational graph to an arbitrary one. In this work, we considered the cycle with periodic boundary conditions. However, the continuous-time quantum walk may behave non-trivially with more complex diagrams. That is why one should consider a general implementation of the walk and the specific charts.

It is worth of the mention that as the variance of the quantum states increases, the number of shots required to obtain the results is expected to increase. Before the practical

quantum advantage in digital quantum simulations, this is a big problem.

Chapter 4

Discrete-time quantum walk

We propose an efficient method for discrete-time quantum walks. Classical methods have shown that Fourier spectral methods can work out a solution to the time-dependent Dirac equation. However, polynomial-time methods remained largely unknown, excluding the discrete-time quantum walk based on adder circuits. In this article, the authors report on a universal tool for computing the spin-1/2 relativistic wave equations (e.g., the Dirac, Majorana, and Weyl equations) based on the first quantized accurate space grid representation using local unitaries. This study utilized the trotterized time evolution at the foundation with Fourier and Walsh-Fourier basis functions to evaluate momentum, mass, scalar, and electromagnetic potential terms on quantum circuits. Our findings demonstrated that the time complexity of several qubits could be reduced to a quadratic for a free particle. It is concluded that the time-dependent relativistic problem, including Zitterbewegung, is now tractable with real devices. This platform creates new opportunities to address the computational challenges of discrete-time quantum walk models.

4.1 Overview

The quantum walk has attracted interdisciplinary fields of quantum sciences accompanied by the quantum speedup, such as exponential speedup for black-box settings and polynomial speedup for several problems of practical interest [42]. One of the remarkable properties is the linear dispersion relation, which distributes the probability amplitude at a bound speed. Moreover, many algorithms have been established with quantum walks owing to properties such as spatial search and Hamiltonian simulations [43, 44]. For the latter, the quantum walk has been generalized to quantum signal processing and quantum singular value transformation [22, 45, 46], which efficiently computes a polynomial transformation to the singular values of the encoded unitary matrix. Moreover, it is shown that the quantum walk can be regarded as a universal computational primitive [47, 48],

where the idea originated from Feynman's first draft of quantum computation.

We usually adopt the finite difference approximation to implement quantum walks classically [49]. This is because the quantum walk is a finite difference equation, and its solution can be obtained straightforwardly through approximation. In this case, the solution is discretized on a regular lattice. While finite difference methods are efficient, numerical errors (such as truncation and interpolation errors) only decay as $1/n^p$ with p-th order finite difference [50].

Another family of numerical methods that use the linear combination of basis functions (such as Fourier, Legendre, and Chebyshev basis) is called spectral methods [51–53]. The methods utilize spectral approximation for evaluating the finite difference equations [54]. In contrast to the former case, the solution is discretized by corresponding polynomials. This situation causes the numerical errors to decay more rapidly than those of finite difference methods in any order such that $1/\log n$, and thus is called an evanescent error [55]. After discovering Cooley and Tukey's fast Fourier transform algorithm [56], a reformed version of the original spectral methods, called pseudospectral methods, was developed [57]. A common approach is to apply the fast Fourier transform and its inverse at each discrete time step. This produces an efficient evaluation of the equations, guaranteeing smooth solutions.

Shor's discovery of the quantum Fourier transform [58] allows us to naturally take advantage of quantum computers for spectral and pseudospectral methods. The circuit complexity of the quantum Fourier transform is known as $O(\log n \log\log n)$ [59], while the complexity of the fast Fourier transform is $O(n \log n)$. This implies that pseudospectral methods can achieve quantum speedup if the trial functions can be efficiently constructed.

Because the continuous-time quantum walk is a discrete analog of the Schrödinger equation, the continuous-time quantum walk algorithm can be developed thoroughly by applying spectral methods to the Schrödinger equation. The work by Kassal *et. al* showed the quantum algorithms with the Fourier pseudospectral method and phase kickback oracle for the first-quantized simulation of the many-body Schrödinger equation [60]. Then it showed that the exponential of trial functions of order k could be implemented with the combination of $O(n^k)$ rotation and controlled rotation gates in the Fourier basis. The state-of-the-art, quantization- and interaction picture-based algorithms are also developed for the simulations [61].

Yet, quantum algorithms for the discrete-time quantum walks, a discrete analog of the Dirac equations, are limited to finite difference approaches. Since the exponential of the spatial derivatives becomes a shift (translation) operator, the quantum circuit can be easily implemented with a stair-like allocation of CNOTs through the approach. However, as mentioned earlier, errors do not decay well in this approach. This becomes

problematic as the scale of quantum computers becomes more extensive, and we desire alternative quantum algorithms for the quantum walks.

In this paper, we show and examine the optimal quantum algorithms based on the Fourier spectral method for the discrete-time quantum walk on a cycle (which gives the periodic boundary conditions) and show that the algorithms can be implemented with two advantages: (1) higher precision, (2) lower CNOT gate count over existing finite-difference schemes. The precision achieved $O(\log(1/\epsilon))$ to simulate the Dirac equation with any vector and scalar potential functions. Furthermore, the computational complexity is reduced to $O(\log n \log\log n)$ for free particles.

We also provide the optimal quantum algorithms for the continuous-time quantum walk on a cycle. While several works focus on the Schrödinger equations, the explicit circuit construction only using CNOTs and single-qubit rotations were unknown. Thus we reconstruct the genetic algorithm with limited gates.

The simulations of continuous- and discrete-time quantum walks are also performed with various settings using classical and quantum computers. Finally, emphasizing that the quantum walks converge to the governing equations in quantum mechanics, we tested our algorithms and simulated their dynamics with specific physical phenomena such as quantum harmonic oscillations, Zitterbewegung, and Klein paradox.

The following is an outline of our paper. In Section 4.2, we define relativistic and nonrelativistic Hamiltonians to derive the continuous- and discrete-time quantum walks to space and time discretizations (Trotter decomposition). Section 3.3 is devoted to providing the quantum algorithm implementation of the continuous-time quantum walk. In contrast, Section 4.3 gives the implementation of the discrete-time quantum walk based on Fourier spectral methods. Both performances are provided by each term of the equations obtained through trotter decompositions. In Section 4.4, we report the numerical analysis of quantum walks and CNOT counts. We then conclude and discuss the simulation results obtained and their possible applications.

4.2 The continuum Hamiltonian

This section focuses on the discretization of the Schrödinger and the Dirac Hamiltonian in $(3+1)$ dimensions. Discretization will be the main ingredient for deriving the quantum spectral methods for continuous- and discrete-time quantum walks. The Dirac Hamiltonian for the Dirac equation in $(3+1)$ dimensions reads

$$H = \boldsymbol{\alpha} \cdot (-i\nabla + e\boldsymbol{A}) + \beta m - e\phi. \tag{4.2.1}$$

$\boldsymbol{\alpha}$ and β are the Dirac matrices interpreted as dimensionless matrices arising from nonrelativistic Hamiltonians' square roots. In this paper, we use the Dirac representation,

where

$$\begin{aligned} \boldsymbol{\alpha} &= \sigma^1 \otimes \boldsymbol{\sigma} \\ \beta &= \sigma^3 \otimes \mathbb{I}_2. \end{aligned} \tag{4.2.2}$$

The set of $\boldsymbol{\sigma} = \sigma^{i=1,2,3}$ are the 2×2 Pauli spin matrices given by

$$\begin{aligned} \sigma^1 &= \quad |0\rangle\langle 1| + \ |1\rangle\langle 0| \\ \sigma^2 &= -i\,|0\rangle\langle 1| + i\,|1\rangle\langle 0| \\ \sigma^3 &= \quad |0\rangle\langle 0| + \ |1\rangle\langle 1| \end{aligned} \tag{4.2.3}$$

with Dirac notation to represent Pauli matrices. Moreover, we have two potential energies; $e\phi$ is the scalar potential, and $e\boldsymbol{A}$ is the external electromagnetic potential. According to [62], there are three ways to impose scalar potentials $e\phi$: Give the term as the zeroth component of a four-vector potential, a scalar term, or a pseudoscalar term. We adopted the first way with the interaction potentials $e\phi = eA_0 + V_{\text{nuc.}}$. Note that we assumed natural units (n.u.).

4.2.1 Time-discretization

We discretize the equation in terms of time to derive the quantum spectral methods for the time-dependent Dirac equation. Namely, we use the product formula (operator splitting) for the time discretization to express the corresponding time evolution operator based on non-commuting Hamiltonians with local Hamiltonians. This procedure is identical to the one found in classical Fourier pseudospectral methods [29–33, 33–35]. Our goal is to find the wave function that has evolved t.

$$|\psi(t)\rangle = \mathcal{T}\left[e^{-i\int_0^t H(s)ds}\right]|\psi(0)\rangle\,. \tag{4.2.4}$$

$\mathcal{T}$ holds the time-ordering of the exponential operators. Now, we think of the explicit discretization of time of the exponentials. In discretization, we approximate the continuous time by the discrete time. In other words, we rewrite the unitary operators as products (that is, the operator splitting) [36–39]. In general, splitting errors arise from the non-commuting terms, but the formula for the $2k$th-order product formula is written by [40]

$$\begin{aligned} \mathscr{S}_2(t) &:= e^{-i\frac{t}{2}\mathbf{A}} \cdot e^{-it\mathbf{B}} \cdot e^{-i\frac{t}{2}\mathbf{A}}, \\ \mathscr{S}_{2k}(t) &:= \mathscr{S}_{2k-2}(u_k t)^2 \mathscr{S}_{2k-2}((1-4u_k)t)\mathscr{S}_{2k-2}(u_k t)^2. \end{aligned} \tag{4.2.5}$$

The product of the exponential operators arrows us to treat the total time evolution operators with local unitaries, with discrete time as the sum of small time steps. As a

result, the original Dirac Hamiltonian is decomposed into the following form.

$$\begin{aligned} H_1 &= -i\boldsymbol{\alpha}\cdot\nabla, \\ H_2 &= \beta m, \\ H_3 &= -e\phi, \\ H_4 &= e\boldsymbol{\alpha}\cdot\boldsymbol{A}. \end{aligned} \tag{4.2.6}$$

Then the time evolution operator for each term can be written as

$$\begin{aligned} \mathscr{S}_2(t) =& e^{-i\frac{t}{2}H_1}\cdot e^{-i\frac{t}{2}H_2}\cdot e^{-i\frac{t}{2}H_3}\cdot e^{-i\frac{t}{2}H_4} \\ & \cdot e^{-i\frac{t}{2}H_4}\cdot e^{-i\frac{t}{2}H_3}\cdot e^{-i\frac{t}{2}H_2}\cdot e^{-i\frac{t}{2}H_1}, \\ \mathscr{S}_{2k}(t) =& \mathscr{S}_{2k-2}(u_k t)^2 \mathscr{S}_{2k-2}((1-4u_k)t)\mathscr{S}_{2k-2}(u_k t)^2. \end{aligned} \tag{4.2.7}$$

As mentioned, the 2nd-order Suzuki-Trotter decomposition guarantees up to 2nd-order in time.

$$\begin{aligned} \left\|\mathscr{S}_2(t) - e^{-itH}\right\| \leqslant & \frac{t^3}{12}\sum_{\gamma_1=1}^{\Gamma}\left\|\left[\sum_{\gamma_3=\gamma_1+1}^{\Gamma} H_{\gamma_3}, \left[\sum_{\gamma_2=\gamma_1+1}^{\Gamma} H_{\gamma_2}, H_{\gamma_1}\right]\right]\right\| \\ & + \frac{t^3}{24}\sum_{\gamma_1=1}^{\Gamma}\left\|\left[H_{\gamma_1}, \left[H_{\gamma_1}, \sum_{\gamma_2=\gamma_1+1}^{\Gamma} H_{\gamma_2}\right]\right]\right\|. \end{aligned} \tag{4.2.8}$$

The details on Trotter errors are elaborated in Ref. [40].

4.2.2 Space-discretization

Next, we think of the spatial discretization of the time-dependent Dirac equation [39, 41]. We need to specify the basis function to derive the quantum spectral methods. While the quantum algorithm for the Chebyshev pseudospectral method is proposed, we have chosen the Fourier basis for convenience and cogency in treating quantum systems. Similarly to time discretization, we take the original continuous domain as the discrete domain with a truncated computational cell volume Ω with n grids. Subsequently, we define the pair:

$$\begin{aligned} r_p &= \frac{p\Omega}{n} && p \in G, \\ k_p &= \frac{2\pi p}{\Omega} && p \in G, \\ G &= \left[-\frac{n-1}{2}, \frac{n-1}{2}\right] && \subset \mathbb{Z}^3. \end{aligned} \tag{4.2.9}$$

Here, r_p is a reciprocal lattice vector at p, and k_p corresponds to the vector in the Fourier space. We note that in Fourier space, the solution is approximated as a linear combination of the trial functions on a Fourier basis. This is the gist of the spectral method, and we will have the spectral (exponential) convergence and accuracy for smooth solutions.

$$\|\psi_h - \psi\| \leqslant n^{s-r}\|\psi\|_{H^s} \quad \text{for } s > r > d/2 \in \mathbb{R}. \tag{4.2.10}$$

4.3 Discrete-time quantum walk

This section shows the explicit quantum circuit of quantum spectral methods for the discrete-time quantum walk. The terms for the implementation include the kinetic $e^{-t\boldsymbol{\alpha}\cdot\nabla}$, the mass energy $e^{-it\beta m}$, the scalar potential energy $e^{iet\phi}$, and the vector potential energy $e^{-iet\boldsymbol{\alpha}\cdot\boldsymbol{A}}$ from Sec. 4.2.

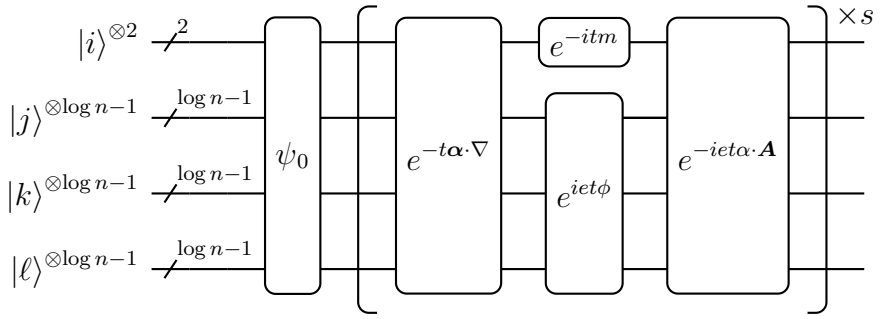

Figure 4.1: Schematic of the quantum spectral method for discrete-time quantum walks. The first block is the initial state preparation block and the next repeating s blocks are the time-splitting operators.

Theorem 4.3.1. *Consider the discrete-time quantum walk on a cycle with the relativistic Hamiltonian defined in (4.2.6). Then for any $t \in \mathbb{R}$ (propagation time) and ϵ (error tolerance) there exists a unitary operation e^{-itH} which can be implemented on quantum computers with complexity*

$$O(\text{poly}(\log(1/\epsilon))). \tag{4.3.1}$$

Again, we begin by defining the quantum registers. Since the spinor of the Dirac equation in $(3+1)$ dimensions, $\psi \in L^2(\mathbb{R}^3) \otimes \mathbb{C}^4$, has $4n^3$ grid points, the number of qubits is given by $\log 4n^3$. We use $\mathscr{Q}_1 - \mathscr{P}_0$ elements where each cell volume is equal, and we get the discretized wave function ψ as summations expressed as

$$\psi = \sum_{i=1}^{4}\sum_{j=1}^{n}\sum_{k=1}^{n}\sum_{\ell=1}^{n} \alpha_{i,j,k,\ell} \left|i\right\rangle \left|j\right\rangle \left|k\right\rangle \left|\ell\right\rangle . \tag{4.3.2}$$

In the following procedure, we elucidate the implementation of the quantum circuit based on quantum spectral methods. The Dirac Hamiltonian 4.2.6 has two sources of nondiagonal elements: the Dirac matrices and the spatial derivative. Unfortunately, both cannot be implemented straightforwardly on a computational basis. However, owing to the property of Pauli matrices and the relation between the coordinate and momentum space, they can be diagonalizable through local unitary operations.

4.3.1 Implementing the kinetic term

Lemma 4.3.2. *For any $t \in \mathbb{R}$ operation $e^{-t\boldsymbol{\alpha}\cdot\nabla}$ can be performed with gate complexity $O(\log n \log\log n)$.*

Proof. We start by diagonalizing the spatial derivative ∇ applying the quantum Fourier transform QFT before and the inverse quantum Fourier transform $\mathrm{QFT}^\dagger$ after differentiation.

$$e^{-t\boldsymbol{\alpha}\cdot\nabla} = (\mathbb{I}_4 \otimes \mathrm{QFT}) e^{it\boldsymbol{\alpha}\cdot\mathbf{p}} (\mathbb{I}_4 \otimes \mathrm{QFT}^\dagger), \tag{4.3.3}$$

where $e^{it\boldsymbol{\alpha}\cdot\mathbf{p}}$ is the kinetic term in the momentum space. In $(3+1)$ dimensions, the term can be expressed as the sum of the three $n \times n$ unitary matrices

$$\begin{aligned} e^{it\boldsymbol{\alpha}\cdot\mathbf{p}} =& e^{it\alpha^1\cdot\mathsf{p}} \otimes \mathbb{I}_n \otimes \mathbb{I}_n \\ &+ \mathbb{I}_n \otimes e^{it\alpha^2\cdot\mathsf{p}} \otimes \mathbb{I}_n \\ &+ \mathbb{I}_n \otimes \mathbb{I}_n \otimes e^{it\alpha^3\cdot\mathsf{p}}. \end{aligned} \tag{4.3.4}$$

with the expression of Dirac matrices [39]

$$\boldsymbol{\Pi} = \frac{1}{\sqrt{2}}(\beta + \boldsymbol{\alpha}). \tag{4.3.5}$$

We begin by representing the discrete variable p in bit form to implement the momentum

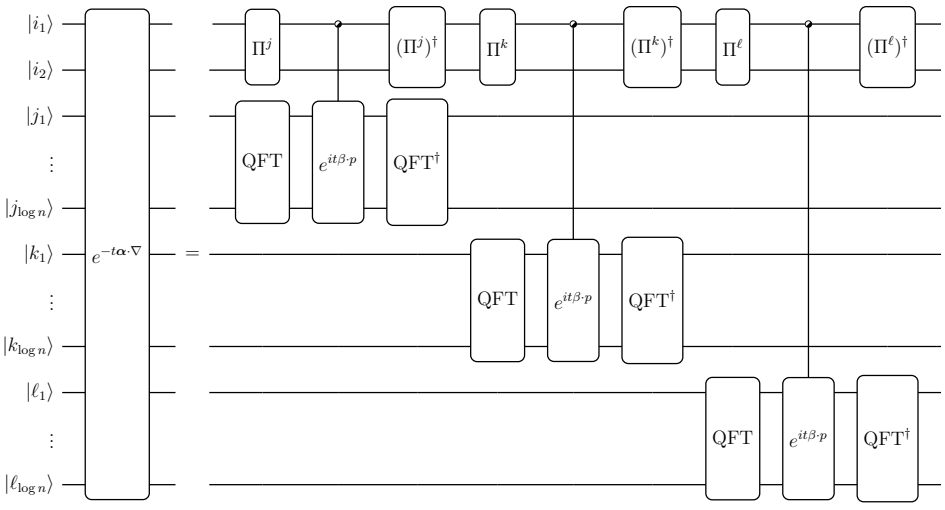

Figure 4.2: Schematic diagram of the alternative direction implicit method. Note that depending on the control, +1 or -1 eigenstate, the direction are reversed.

operator.

$$p = -\frac{2\pi}{\Omega} \sum_{j=1}^{\log n} 2^j Z_j. \tag{4.3.6}$$

A diagonal linear, exponential operator similar to the one used in [63] can be implemented using single-qubit gates from $O(\log(n))$. Since Pauli matrix α exists in the momentum operator, we have the fixed Z gate on 0-th qubit. As a result, we have the following.

$$e^{it\alpha\cdot\mathfrak{p}} = (\Pi \otimes \mathbb{I}_{n-4}) e^{it\beta\cdot p} (\Pi^\dagger \otimes \mathbb{I}_{n-4}). \tag{4.3.7}$$

As can be seen, the exponential on the right-hand side of the equation can be imple-

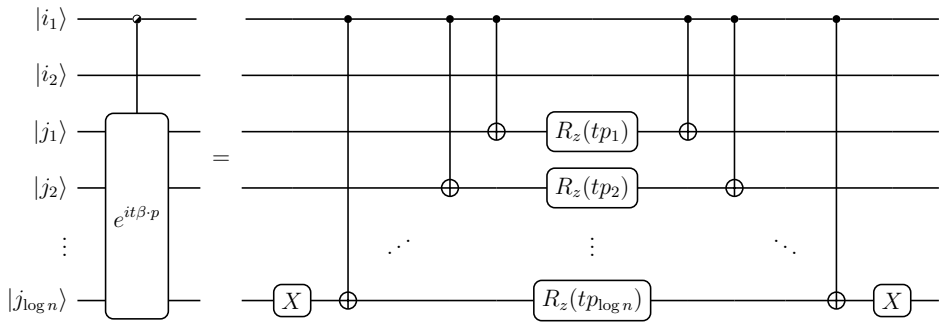

Figure 4.3: Quantum circuit for the momentum operator applied to two-spinor Dirac wave function on $\log n$ qubits.

mented in the gate sequence R_z. The products of Z_1 and Z_j in the Eq. (4.3.7) reflect the momentum operations in bispinor spaces. Fig. (4.2) is the quantum circuit corresponding to the Eq. (4.3.7). CNOT gates interpose the single qubit rotations to add degrees of freedom [64]. Besides, the X gates at the beginning and end are used to shift the momentum space into the center [65].

It was investigated that the stability of the term is the following inequality.

$$\left\| e^{it\alpha\cdot p}\psi(0) - \psi(t) \right\|_{H^s} \leqslant t^2 C \|\psi(0)\|_{H^{s+2}}. \tag{4.3.8}$$

Moreover, consistency is also guaranteed with the Sobolev norm.

$$\left\| e^{it\alpha\cdot p}\psi(0) \right\|_{H^s}^2 = \|\psi(0)\|_{H^{s+2}}^2. \tag{4.3.9}$$

Since convergence and stability are known, convergence can also be derived from the Lax-Richtmyer equivalence theorem.

$$\left\| e^{is\alpha\cdot p}(T/s)\psi(0) - e^{it\alpha\cdot\mathfrak{p}}\psi(0) \right\|_{H^s} \leqslant sTC \|\psi(0)\|_{H^{s+2}}. \tag{4.3.10}$$

As can be seen, the shift matrix can achieve spectral convergence. □

4.3.2 Implementing the mass term

Lemma 4.3.3. *The quantum circuit $e^{-it\beta m}$ can be performed with gate complexity $O(1)$.*

Proof. In this subsection, we consider implementing the mass term.

$$e^{-it\beta m} = e^{-itmZ} \otimes \mathbb{I}_{n-2}. \tag{4.3.11}$$

The mass operator defined in the last section is an exponential of the constants and the Dirac matrix β. Thus, the operation can be absorbed into a single-qubit rotation.

$$e^{-itmZ} \otimes \mathbb{I}_{n-2} \equiv |j_0\rangle \quad \text{—} \boxed{R_z(2tm)} \text{—} \cdot \tag{4.3.12}$$

While the mass operator is a single-qubit rotation, it runs on all the qubits. This is because when the rotation is applied to the spinor register $|s\rangle$, the identity gates $\mathbb{I}$ are turned to all the space registers $|j\rangle$. □

4.3.3 Implementing the scalar potential term

Lemma 4.3.4. *The quantum circuit $e^{iet\phi}$ with error tolerance ϵ can be performed with gate complexity $O(\mathrm{poly}(\log(1/\epsilon)))$.*

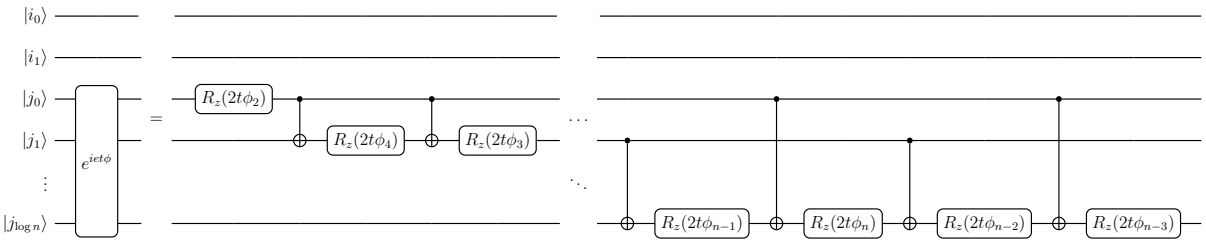

Figure 4.4: Quantum gate decomposition for arbitrary $e^{iet\phi}$ Hamiltonian based on Walsh operators for Schrödinger-like (one-spinor) wave function proposed in [1].

Proof. The upcoming implementation is the scalar and electromagnetic potentials. As noted in [39], the scalar potential requires us to implement space-dependent exponential functions (or phase operations).

$$e^{iet\phi} \equiv \mathbb{I}_4 \otimes e^{iet\phi}. \tag{4.3.13}$$

Similarly, we assume that the electromagnetic potential depends on space-dependent phase operations for general applications. It is well known that the diagonal unitary

transform consumes $n-3$ gates [66] that come from the oracle. Therefore, if the function has some structure, the gate count can be reduced to $O(\text{poly}(\log(n)))$. Moreover, given discrete Walsh transform,

$$-\phi_m = -\int dx \phi \omega_m. \tag{4.3.14}$$

Here, we start by constructing the scalar potential, which is straightforward relative to the energy of the electromagnetic potential. In $\log n$ qubits register, j-th Walsh operator ω_m can be constructed using sum of Z gates

$$\begin{aligned} -e\phi &\approx -\sum_{m=1}^{n} \phi_m \omega_m, \\ &= -\sum_{m=1}^{n} \sum_{j=1}^{\log n} \phi_m 2^j Z_j^{m_j} \quad m_j = \left\lfloor \frac{m}{2^j} \right\rfloor - 2\left\lfloor \frac{m}{2^{j+1}} \right\rfloor. \end{aligned} \tag{4.3.15}$$

The quantum circuit implementation for the scalar potential can easily be derived using the Walsh coefficients obtained from the discrete Walsh transform and its quantum circuit representation. Note that this operator does not act on the spinor register $|s\rangle$ but on the space report $|j\rangle$.

In the following, we describe the approximation of the Walsh-Fourier series to achieve the polynomial time complexity. Given an exact potential energy $-e\phi$, we consider an approximated one within the error.

$$|e\phi - e\phi_\epsilon| \leqslant \epsilon. \tag{4.3.16}$$

Subsequently, the supreme norm of the approximation is given as

$$\epsilon_\phi = \sup_G |e\phi - e\phi_\epsilon| \leqslant \frac{\sup_G |-e\phi'|}{n'}, \tag{4.3.17}$$

where n' is the number needed for a new function. Consequently, we reach the following error as a total,

$$\left\| e^{iet\phi} - e^{iet\phi_\epsilon} \right\| \leqslant \epsilon \quad \text{for } \epsilon_\phi \leqslant \epsilon, \tag{4.3.18}$$

which automatically guarantees the polynomial complexity. □

4.3.4 Implementing the vector potential term

Lemma 4.3.5. *The quantum circuit $e^{-iet\boldsymbol{\alpha}\cdot\boldsymbol{A}}$ with error tolerance ϵ can be performed with gate complexity $O(\text{poly}(\log(1/\epsilon)))$.*

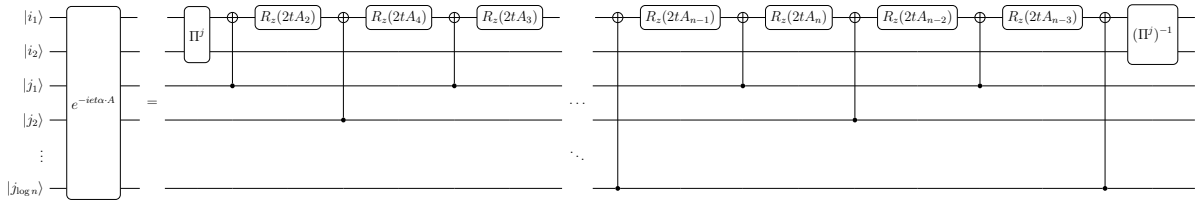

Figure 4.5: Quantum circuit for arbitrary $e^{-iet\boldsymbol{\alpha}\cdot\boldsymbol{A}}$ Hamiltonians based on the row-wise Walsh operators for two-spinor Dirac wave function on three qubits. The diagonal unitary transformation is computed on two spinors with opposite phases $\mathrm{diag}(\theta_i, -\theta_i)$.

Proof. The final operator to implement is the electromagnetic potential energy term. The difference between the scalar and the electromagnetic potential is the presence of the Dirac matrices $\boldsymbol{\alpha}$. Then, we apply the circuit identity again to compute the matrix on a computational basis. Finally, we obtain the diagonal unitaries using the identity on the Z basis.

$$e^{-iet\alpha\cdot A} = (\Pi \otimes \mathbb{I}_{n-4}) e^{-ietAZ_1Z_2} (\Pi^\dagger \otimes \mathbb{I}_{n-4}) \tag{4.3.19}$$

An efficient way to implement the function A is to evaluate it on a Walsh basis. Walsh coefficients a_m are obtained from the Walsh transform.

$$A_m = \int dx A\omega_m. \tag{4.3.20}$$

Having the coefficients, we can now implement the electromagnetic potential function as the sequence of quantum gates.

$$\begin{aligned} A &\approx \sum_{m=1}^{n} A_m \omega_m, \\ &= \sum_{m=1}^{n} \sum_{j=1}^{\log n} A_m 2^j Z_j^{m_j} \quad m_j = \left\lfloor \frac{m}{2^j} \right\rfloor - 2\left\lfloor \frac{m}{2^{j+1}} \right\rfloor. \end{aligned} \tag{4.3.21}$$

Walsh basis representation of objective functions in quantum registers can be efficiently implemented using resampling and suppressed errors $O(1/\epsilon)$ [1]. That is, n' Walsh functions are taken from complete n Walsh functions such that $n' \leqslant n$. And the resampled Walsh is defined as follows. Accordingly, the absolute error is determined by the relation to the 2^k samples such that

$$|eA_\epsilon - eA| \leqslant \epsilon, \tag{4.3.22}$$

with

$$\epsilon_A = \sup_G |eA_\epsilon - eA| \leqslant \frac{\sup_G |A'|}{n'}. \tag{4.3.23}$$

Consequently, this implies that having the absolute error $\epsilon_A \leqslant \epsilon$, the number of Walsh functions required to approximate the function f is $O(1/\epsilon)$.

$$\left\| e^{-iet\alpha \cdot A} - e^{-iet\alpha \cdot A_m} \right\| \leqslant \epsilon \quad \text{for } \epsilon_A \leqslant \epsilon. \tag{4.3.24}$$

□

4.4 Simulation results

We start by testing the algorithm with Zitterbewegung, known for the trembling motion of the Dirac wave packet. We set the initial spinor

$$\psi_0^{\pm}(x) = \exp\left(-\frac{x^2}{2} + ik_0 x\right), \tag{4.4.1}$$

where $k_0 = 1/4$ and consider a massive free Dirac particle, where we assume $A_1 = V = 0$ with $\hbar = c = 1$. The spinor with a Gaussian initial state has both of the two components. The positive and negative parts of the spinor are localized in the momentum space to contribute to the Zitterbewegung phenomenon. Fig. 4.6 shows the expectation value of the position in the total time evolution 1.5×10^{-1} n.u. divided by 100-time steps with different mass parameters from $m = 0$ to $m = 10$. When the mass is $m = 0$, the corresponding velocity is the speed of light. On the other hand, as the mass increases, the Dirac particle starts to move laterally, reflecting the trembling motion.

The next experiment is devoted to evaluating the potential operator of the algorithm. It is known that the different order of Walsh functions (e.g., dyadic order) results in different circuits while keeping the equivalence. However, this implies the same circuit will appear after the CNOT optimization. For example, due to the property of Walsh basis, the step potential shown can be absorbed into a single-qubit rotation gate

$$e^{-itV_0} = |j_1\rangle \quad \boxed{R_z(tV_0)} \quad , \tag{4.4.2}$$

After optimization. Next, we define the (Hartree) atomic units. In atomic units, it is assumed that $\hbar = m = e = 4\pi\epsilon_0 = 1$, where m is the mass of the electron, e is the charge of the electron and ϵ_0 the permittivity of the vacuum. In addition, the speed of light is derived from the dimensionless fine-structure constant.

$$\alpha = \frac{e^2}{4\pi\epsilon_0 \hbar c} \quad c = \frac{1}{\alpha}. \tag{4.4.3}$$

We then set the initial wave packet according to [67]

$$\psi_0^{+}(z) = \mathcal{N} e^{ipz_0} e^{-(p-p_0)^2 \delta z^2} w_p^{+}(z) \tag{4.4.4}$$

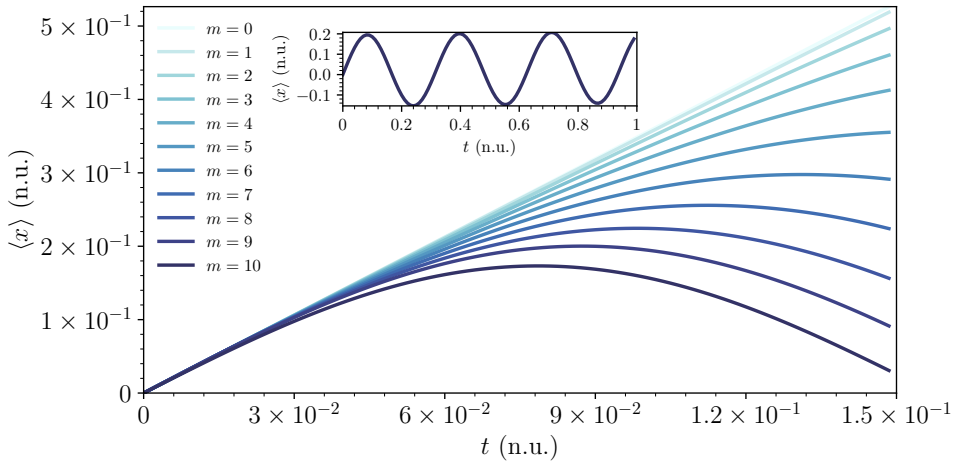

(a)

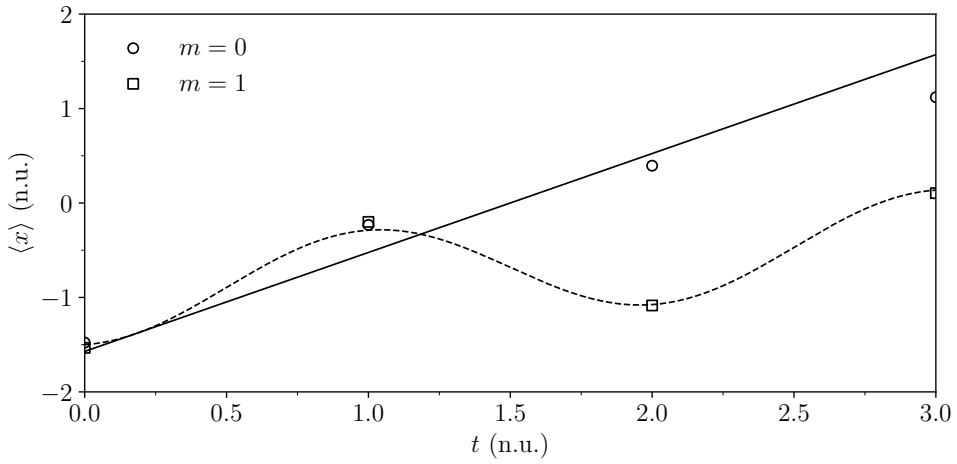

(b)

Figure 4.6: One-dimensional simulation of the Zitterbewegung by the quantum pseudospectral method. The expectation value $\langle x \rangle$ shown on the graph tells us that the Dirac particle starts the trembling motion as the mass m increases.

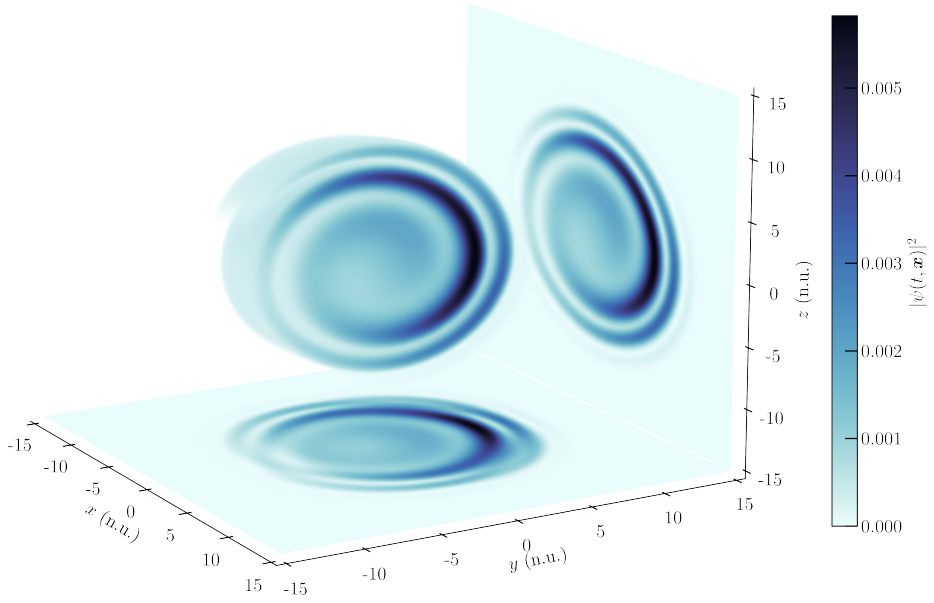

Figure 4.7: Classically emulated three-dimensional quantum simulation of the Zitterbewegung. Initial wave function is distributed around $x, y, z = 0$ with the particle mass $m = 1$. The mass gives the rotation of the wave function which is clearly shown in the plot.

where $\mathcal{N}$ is the normalization constant, $\delta z = 0.03$ a.u. is the initial spatial width, and $p_0 = 106.4$ a.u. is the central momentum. In Fig. 4.8, we show the time evolution of positive eigenstates as an initial wave packet divided into 512 steps from $t = 0$ to $t = 6.82 \times 10^{-3}$. Since the step potential is in the center, at the moment the distribution of the packet on the right-hand side reached the center, it hit the potential wall, and the interference pattern appeared. When the wave packet transmits to the right region, Klein pair production occurs so that it transforms into the antiparticle.

Next, we plot the CNOTs required to simulate the one-dimensional relativistic and non-relativistic system solved via quantum spectral methods for the single time step in Fig. 4.9. It shows that the CNOTs are required less in simulating single-particle Dirac, Weyl, and Majorana equations than the Schrodinger equation. In terms of implementation, this is because the second-order differentiation is more expensive than the Dirac operation (square root of the differentiation). However, the overall complexity of both quantum algorithms is $O(n^2)$.

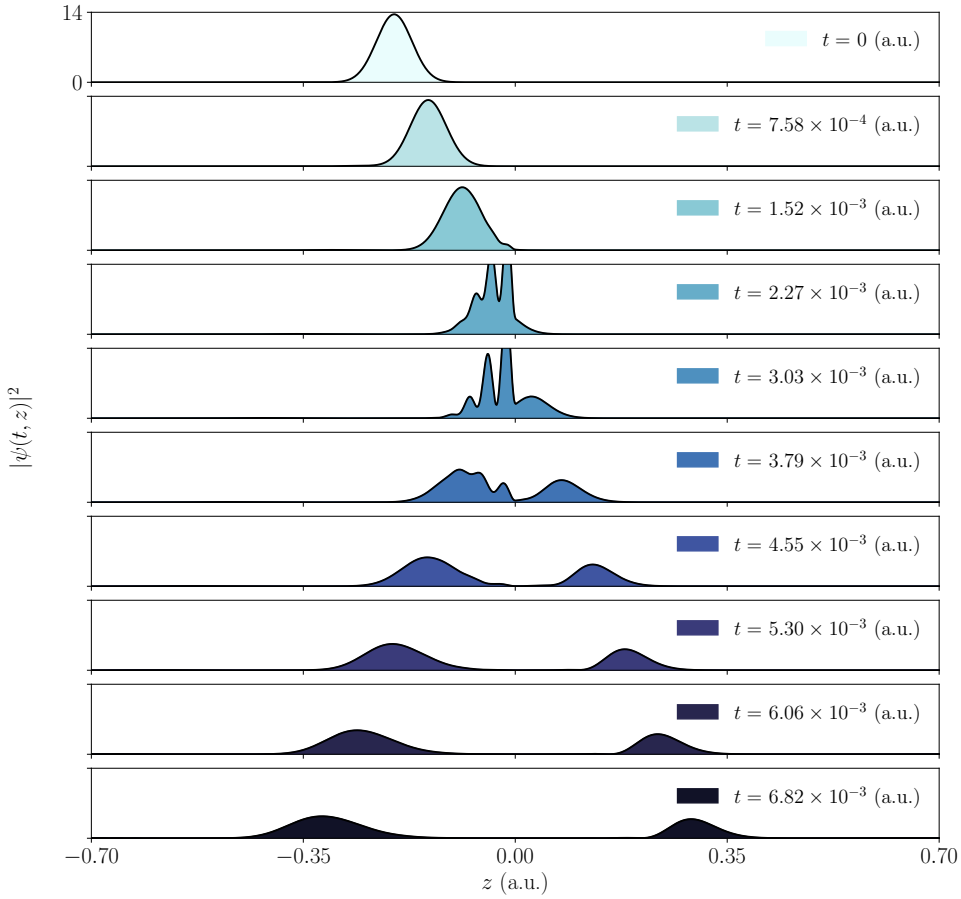

Figure 4.8: One-dimensional simulation of the Klein paradox by the quantum pseudospectral method. Electron wave packet hit on a step potential in the order of electron mass, which is located in the center $z = 0$. After the scattering, the incoming wave is reflected and transmitted with weights of 0.6452 and 0.3542. We used a total of 11 qubits in the simulation.

In 4.10, we tested the convergence of the shift operator with quantum (Fourier) spectral and finite difference methods. Similarly to the continuous-time quantum walk, we see the quantum spectral method's exponential (spectral) convergence due to the Fourier domain evaluation.

4.5 Conclusions & discussion

This paper considers the quantum circuit implementation and the digital quantum simulation of the discrete-time quantum walk with various settings. The primary research question was the development of efficient quantum algorithms for the discrete-time quantum walk. Compared to the previous research, which is done by finite-difference methods,

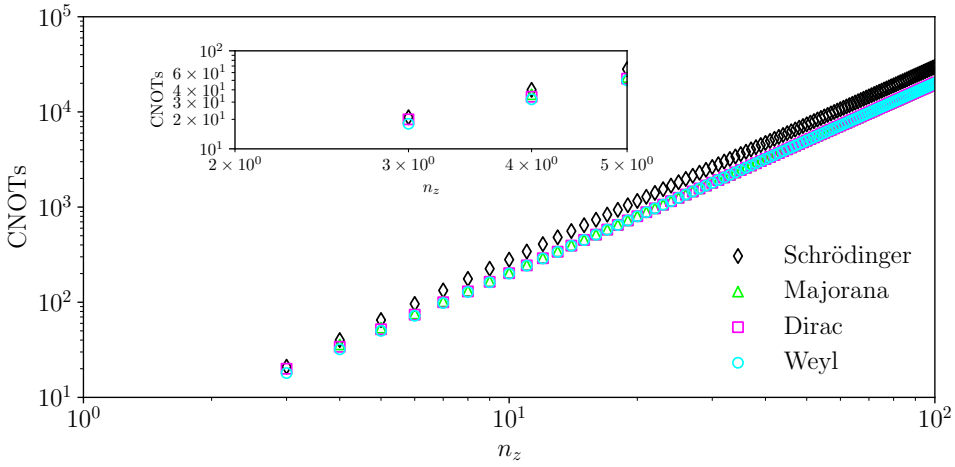

Figure 4.9: CNOT gate counts for the one-dimensional relativistic and non-relativistic system solved via quantum spectral methods. The horizontal axis shows the number of qubits n_z for the z direction. With 10^2 qubits the single time step the number of CNOTs are proportional to 10^4.

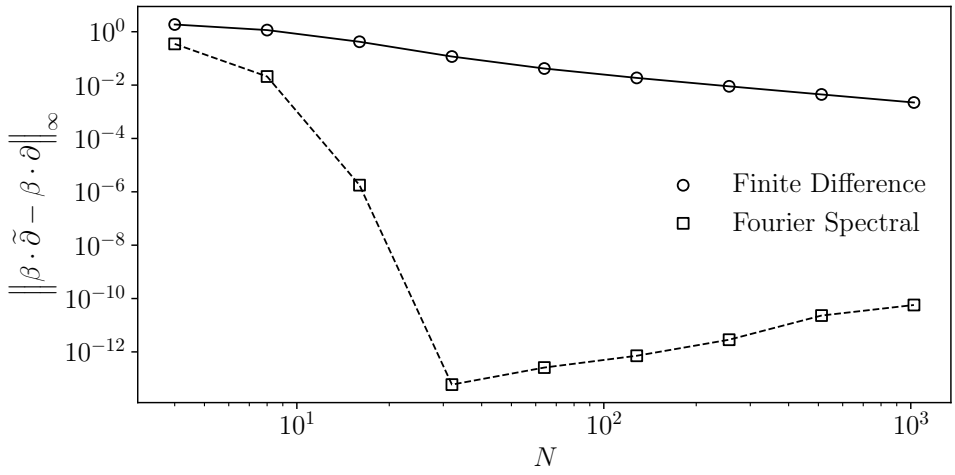

Figure 4.10: log-scale plot of the error estimate of the 1st-order differential operator. The horizontal axis shows the number of grid points in a single dimension while the vertical axis show the convergence rate. The plot shows spectral convergence.

we could reduce the order of the number of CNOTs required for simulating a one-time step. Moreover, we can interpret the reduction as a result of the best-known gate complexity of the quantum Fourier transform being better than multi-CNOTs. But we note that the overall time complexity is the same in both situations.

Extending the discrete-time walk to a general relativistic spacetime is attractive for future work, i.e., the discrete model for the Dirac equation in curved spacetime. The model is partially proposed and simulated on classical computers, but the fully 3+1 dimensional model has not been submitted. Moreover, it is known that the family of the quantum walk gives non-homogeneous dynamics. Therefore, it is physically attractive as well.

Chapter 5

Discrete-spacetime quantum walk

Quantum simulations have been proposed on quantum computers, whereas general relativity has been explored mainly on classical supercomputers. Although a unified understanding of quantum and gravity is one of the most critical subjects in physics, only a few numerical studies have been made at this intersection. Therefore, we propose using quantum computers to simulate quantum dynamics in classical gravitational fields. Specifically, we formulate the $(3+1)$ dimensional Dirac equation in curved spacetime as a discrete spacetime quantum walk. This model makes it possible to reproduce the dynamics of elementary particles in semi-classical gravitational fields, such as fermion tunneling from a dynamical horizon. Furthermore, we give the components for the simulation of charged carriers in graphene that appear in condensed matter physics. This work is expected to be a prominent tool for simulating quantum dynamics coupled with classical gravity.

5.1 Overview

One of physics's most important subjects is a unified understanding of quantum and gravity [68]. However, at the Planck scale, where the quantum mechanics, relativity, and gravity are related, the quantum field theory becomes nullified due to the non-renormalizability of gravity [69].

Quantum computers have been investigated for their ability to solve quantum mechanical problems in a way that supercomputers cannot. As the analytical derivation becomes infeasible, physically attractive quantum systems appear with a super-large number of particles and spacetime points [70]. Quantum computers can handle such systems much more accessible than classical computers, as the qubits also increase the dimensions of Hilbert space exponentially.

On the other hand, it remains to be seen whether the advantages of quantum computation can be extended to gravity, a vastly different physics scale. For instance, quantum theory lies under Planck's constant $h = 6.626 \times 10^{-34}$ J $\cdot$ s, while the special relativity is around the speed up light $c = 299,792,458$ m $\cdot$ s^{-1}, and the gravitational constant for general relativity is 6.674×10^{-11} m^3 $\cdot$ kg^{-1} $\cdot$ s^{-2}. This implies that there is a "big desert" between the two theories.

In the following, we show that a quantum computer can efficiently simulate the dynamics of a spin-1/2 particle with semiclassical gravity, which approximates the quantum gravity by the classical treatment of the gravitational fields.

5.2 The continuum Hamiltonian

To couple semiclassical gravity with the Dirac equation, we define the time-dependent Dirac equation in curved spacetime. In the natural unit, it is written as [71]

$$\Big[i\gamma^\mu(\partial_\mu + \Omega_\mu - ieA_\mu) - m\Big]\psi = 0. \tag{5.2.1}$$

The main difference from the balanced equation is the spacetime-dependent matrices γ^μ and the affine spin connection Ω_μ. The former is related via tetrad formalism to induce the gravitational effects, while the latter is introduced to preserve the covariance. We aim to simulate the dynamics governed by Eq. (5.2.1) on quantum computers. On the contrary, Schrödinger-form of the equation is not Hermitian in a general case, as the self-conjugation of the affine spin connection is not. Thus, we transform into the Hermitian form [72]

$$\psi' = \gamma^{1/4}\psi, \tag{5.2.2}$$
$$H' = \gamma^{1/4} H \gamma^{-1/4}, \tag{5.2.3}$$

where $\gamma = \det(\gamma_{ij})$ with respect to the scalar product. In addition, coordinate singularities will be problematic as they arise non-unitarity in the time evolution. For this purpose, we introduce the $(3+1)$ formalism used in numerical relativity. Then the line element can be written as

$$ds^2 = \alpha^2 dt^2 - \gamma_{ij}(dx^i + \beta^i dt)(dx^j + \beta^j dt) \tag{5.2.4}$$

As a result, Eq. (5.2.1) becomes following Hamiltonian equation

$$i\partial_t \left|\psi'(t)\right\rangle = H' \left|\psi'(t)\right\rangle, \tag{5.2.5}$$

with the Hamiltonian H'

$$\begin{aligned} H' = &- i(\gamma^0\gamma^j e_j{}^i\alpha - \beta^i)(\partial_i + \Omega_i - ieA_i) \\ &+ \gamma^0 m\alpha - \mathbb{I}_4(i\Omega_0 + eA_0). \end{aligned} \tag{5.2.6}$$

5.3 Discrete-spacetime quantum walk

To simulate the dynamics of the Dirac equation in curved spacetime, we first discretize it as a quantum walk. It is well known that the discrete-time quantum walk can be considered a discrete analog of the Dirac equation in Minkowski spacetime with its non-commutativity of the time evolution operator. Since we are deriving a quantum walk from a general spacetime metric, we should call our subject the discrete-spacetime quantum walk concerning the Dirac equation in curved spacetime. In any case, the goal of simulating quantum dynamics is to find the evolution over time t,

$$|\psi'(t)\rangle = \mathcal{T}\left[e^{-i\int_0^t H'(s)\mathrm{d}s}\right]|\psi'(0)\rangle\,, \tag{5.3.1}$$

where $\mathcal{T}$ holds the time-ordering.

5.4 Simulation results

In Figure 5.1, we show the simulation results obtained by a Python framework for quantum computation known as Qiskit. In the classically emulated quantum simulation, nine qubits are used for the spatial resolution, and a qubit is consumed for the spin degrees of freedom. The spacetime is assumed as a Schwarzschild black hole situation of the mass $M = 0.5$ with a massless Dirac particle. The metric tensor of the system is given as

$$g = -\left(\frac{1-m/2\bar{r}}{1+m/2\bar{r}}\right)^2 + \left(1+\frac{m}{2\bar{r}}\right)^4 (d\bar{r}^2 + \bar{r}^2 d\theta^2 + \bar{r}^2\sin^2\theta d\varphi) \tag{5.4.1}$$

5.5 Conclusions & discussion

In this work, we formulated quantum simulations in curved spacetime by deriving the discrete-spacetime quantum walk from scratch. Since this approach is deductive in contrast to the previous inductive research, we could reveal the algorithmic extensions needed for the quantum walk in discrete-spacetime. Specifically, we found that the ordinary shift operator of the Dirac equation is reminiscent of flat spacetime. That is, two coins and shift operators are required to include the spacetime's curvature.

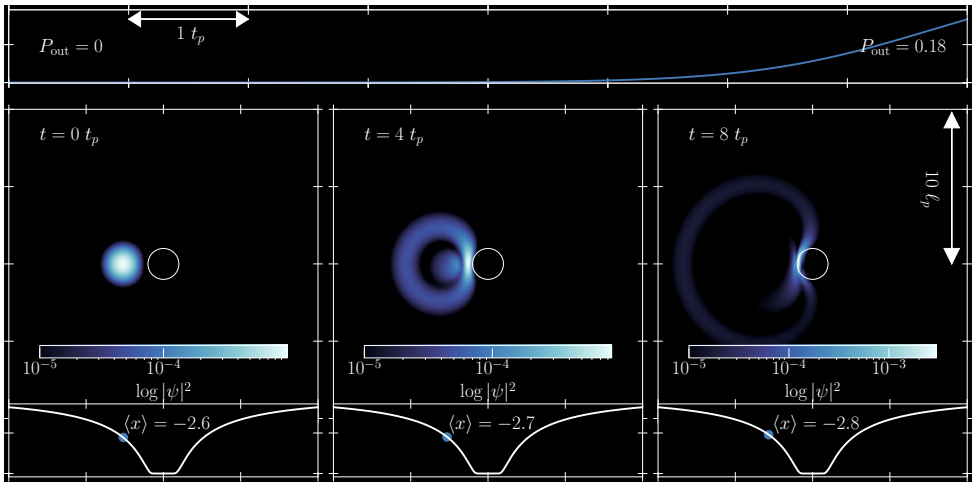

Figure 5.1: Classically emulated one-dimensional quantum simulation results of discrete-spacetime quantum walk in Schwarzschild spacetime. Schwarzschild black hole is allocated around the origin and it creates the curvature of the spacetime via gravitational effects.

Chapter 6

Conclusion

In this thesis, we introduced the continuous-time, discrete-time, and discrete-spacetime quantum walk algorithms with their efficient implementations by quantum spectral methods. Generally, it is essential to distinguish the usage of every numerical scheme. This is because each numerical techniques have advantages and disadvantages. For example, the most famous numerical method, the finite-difference method, is straightforward to implement the plan. However, on the other hand, the numerical errors only decrease in proportion to the spatial resolution. On the contrary, spectral methods are not that straightforward to implement, but the errors decrease exponentially to the spatial resolution. Thus we can conclude that in the situation of NISQ with a few qubits, we would like to utilize the property of spectral methods, as suppressing the error is a critical task in that regime.

Of course, it is also essential to consider the types of target systems in distinguishing the numerical methods. Our primary focus was on semiclassical quantum gravity, where the matter is quantum while the gravity is classical. In cases where unitary operations give the evolution, the solution is always continuous. That is why we can take advantage of spectral convergence accompanied by spectral methods.

Several additional works must be placed toward the full simulation of the semiclassical quantum gravity. First, it is preferred to be able to crop the coordinate singularity. In a black hole spacetime, it emerges where the gravitational effects are too strong. In such cases, numerical treatments become extremely difficult as the solutions go to infinity. While there has not been a concrete proposal, the so-called perfectly matched layer is a critical technique that may solve this problem. The perfectly matched layer is an absorption layer that is facilitated at boundaries. If periodic boundary conditions are imposed, the solution usually appears at the opposite edge after passing a border. However, if the layer is allocated, the answer is absorbed when it comes close to the edge. This indicates that if we can formulate the coating around the coordinate singularity, we can avoid the

key reaching infinity. That is why it is desired to be explored in a certain depth.

Second, since we only focused on quantum mechanics, it is interesting to employ canonical quantization. In quantum gravity, we not only consider both matter and gravity as quantum but also assume both of them are fields. In this work, matter is a single particle, meaning it is not a field.

Simulating the time-dependent Dirac equation on a quantum computer can also be extended to a simulation of the lattice gauge theories. In lattice gauge theories, a generalized version of the Dirac equation called the Dirac operator appears. It described the matter (quarks) on a lattice field. However, the operator is computationally very expensive, as the degrees of freedom are more than a Dirac equation due to the existence of colors from quantum chromodynamics. Moreover, while there is a strong motivation regarding the computational complexities, as mentioned, the Dirac operator is not a Hamiltonian, meaning it is not Hermitian. Since it is not Hermitian, we must devise a way to treat it in a unitary framework. Recently, a unitary framework of a single-particle lattice gauge theory has been proposed. This approach uses the discrete-time quantum walk to evaluate Wilson's fermions. This method, however, suffers from fermion doubling problems. Thus, much work is still needed to realize its quantum simulation.

Bibliography

[1] J. Welch, D. Greenbaum, S. Mostame, and A. Aspuru-Guzik, "Efficient quantum circuits for diagonal unitaries without ancillas," *New Journal of Physics* **16** no. 3, (Mar, 2014) 033040. http://dx.doi.org/10.1088/1367-2630/16/3/033040.

[2] P. A. M. Dirac, *The principles of quantum mechanics*. No. 27. Oxford university press, 1981.

[3] A. Einstein, *Relativity*. Routledge, 2013.

[4] N. Ashby, "Relativity in the global positioning system," *Living Reviews in Relativity* **6** no. 1, (Jan., 2003) 1.

[5] A. G. J. MacFarlane, J. P. Dowling, and G. J. Milburn, "Quantum technology: the second quantum revolution," *Philosophical Transactions of the Royal Society of London. Series A: Mathematical, Physical and Engineering Sciences* **361** no. 1809, (2003) 1655–1674. https://royalsocietypublishing.org/doi/abs/10.1098/rsta.2003.1227.

[6] W. Rindler, "Relativity: special, general, and cosmological." 2003.

[7] A. Steane, "Quantum computing," *Reports on Progress in Physics* **61** no. 2, (Feb, 1998) 117. https://dx.doi.org/10.1088/0034-4885/61/2/002.

[8] R. P. Feynman, "Simulating physics with computers," *International Journal of Theoretical Physics* **21** no. 6, (June, 1982) 467–488.

[9] D. Deutsch and R. Penrose, "Quantum theory, the church–turing principle and the universal quantum computer," *Proceedings of the Royal Society of London. A. Mathematical and Physical Sciences* **400** no. 1818, (1985) 97–117. https://royalsocietypublishing.org/doi/abs/10.1098/rspa.1985.0070.

[10] I. M. Georgescu, S. Ashhab, and F. Nori, "Quantum simulation," *Rev. Mod. Phys.* **86** (Mar, 2014) 153–185. https://link.aps.org/doi/10.1103/RevModPhys.86.153.

[11] I. Buluta and F. Nori, "Quantum simulators," *Science* **326** no. 5949, (2009) 108–111. https://www.science.org/doi/abs/10.1126/science.1177838.

[12] B. C. Travaglione and G. J. Milburn, "Implementing the quantum random walk," *Phys. Rev. A* **65** (Feb, 2002) 032310. https://link.aps.org/doi/10.1103/PhysRevA.65.032310.

[13] A. M. Childs, "On the relationship between continuous- and Discrete-Time quantum walk," *Communications in Mathematical Physics* **294** no. 2, (Mar., 2010) 581–603.

[14] C. M. Chandrashekar, S. Banerjee, and R. Srikanth, "Relationship between quantum walks and relativistic quantum mechanics," *Physical Review A* **81** no. 6, (Jun, 2010) . https://doi.org/10.1103%2Fphysreva.81.062340.

[15] P. Arrighi, V. Nesme, and M. Forets, "The dirac equation as a quantum walk: higher dimensions, observational convergence," *Journal of Physics A: Mathematical and Theoretical* **47** no. 46, (Nov, 2014) 465302. https://doi.org/10.1088%2F1751-8113%2F47%2F46%2F465302.

[16] D. M. Giuseppe, F. Debbasch, and M. E. Brachet, "Quantum walks as massless dirac fermions in curved space-time,". https://arxiv.org/abs/1212.5821.

[17] P. Arrighi, S. Facchini, and M. Forets, "Quantum walking in curved spacetime." 2015. https://arxiv.org/abs/1505.07023.

[18] D. ben Avraham, E. M. Bollt, and C. Tamon, "One-dimensional continuous-time quantum walks," *Quantum Information Processing* **3** no. 1, (Oct, 2004) 295–308. https://doi.org/10.1007/s11128-004-9420-8.

[19] S. Lloyd, "Universal Quantum Simulators," *Science* **273** no. 5278, (Aug., 1996) 1073–1078.

[20] A. M. Childs and N. Wiebe, "Hamiltonian simulation using linear combinations of unitary operations," *Quantum Info. Comput.* **12** no. 11–12, (Nov, 2012) 901–924.

[21] D. W. Berry and A. M. Childs, "Black-box hamiltonian simulation and unitary implementation," *Quantum Info. Comput.* **12** no. 1–2, (Jan, 2012) 29–62.

[22] G. H. Low and I. L. Chuang, "Optimal hamiltonian simulation by quantum signal processing," *Phys. Rev. Lett.* **118** (Jan, 2017) 010501. https://link.aps.org/doi/10.1103/PhysRevLett.118.010501.

[23] G. H. Low and I. L. Chuang, "Hamiltonian simulation by qubitization," *Quantum* **3** (Jul, 2019) 163. https://doi.org/10.22331%2Fq-2019-07-12-163.

[24] A. M. Childs and J. Goldstone, "Spatial search by quantum walk," *Phys. Rev. A* **70** (Aug, 2004) 022314. https://link.aps.org/doi/10.1103/PhysRevA.70.022314.

[25] M. Feit, J. Fleck, and A. Steiger, "Solution of the schrödinger equation by a spectral method," *Journal of Computational Physics* **47** no. 3, (1982) 412–433. https://www.sciencedirect.com/science/article/pii/0021999182900912.

[26] M. R. Hermann and J. A. Fleck, "Split-operator spectral method for solving the time-dependent schrödinger equation in spherical coordinates," *Phys. Rev. A* **38** (Dec, 1988) 6000–6012. https://link.aps.org/doi/10.1103/PhysRevA.38.6000.

[27] M. Thalhammer, M. Caliari, and C. Neuhauser, "High-order time-splitting hermite and fourier spectral methods," *Journal of Computational Physics* **228** no. 3, (2009) 822–832. https://www.sciencedirect.com/science/article/pii/S0021999108005251.

[28] M. Dehghan and A. Taleei, "Numerical solution of nonlinear schrödinger equation by using time-space pseudo-spectral method," *Numerical Methods for Partial Differential Equations* **26** no. 4, (2010) 979–992. https://onlinelibrary.wiley.com/doi/abs/10.1002/num.20468.

[29] C. Bottcher and M. R. Strayer, "Numerical solution of the time-dependent dirac equation with application to positron production in heavy-ion collisions," *Phys. Rev. Lett.* **54** (Feb, 1985) 669–672. https://link.aps.org/doi/10.1103/PhysRevLett.54.669.

[30] G. R. Mocken and C. H. Keitel, "Fft-split-operator code for solving the dirac equation in 2+1 dimensions," *Computer Physics Communications* **178** no. 11, (2008) 868–882. https://www.sciencedirect.com/science/article/pii/S0010465508000611.

[31] G. R. Mocken and C. H. Keitel, "Quantum dynamics of relativistic electrons," *Journal of Computational Physics* **199** no. 2, (2004) 558–588. https://www.sciencedirect.com/science/article/pii/S0021999104000956.

[32] K. Momberger, A. Belkacem, and A. H. So/rensen, "Numerical treatment of the time-dependent dirac equation in momentum space for atomic processes in relativistic heavy-ion collisions," *Phys. Rev. A* **53** (Mar, 1996) 1605–1622. https://link.aps.org/doi/10.1103/PhysRevA.53.1605.

[33] H. Bauke and C. H. Keitel, "Accelerating the fourier split operator method via graphics processing units," *Computer Physics Communications* **182** no. 12, (2011)

2454–2463.
https://www.sciencedirect.com/science/article/pii/S0010465511002414.

[34] W. Bao and X.-G. Li, "An efficient and stable numerical method for the maxwell–dirac system," *Journal of Computational Physics* **199** no. 2, (2004) 663–687.
https://www.sciencedirect.com/science/article/pii/S0021999104001111.

[35] J. Xu, S. Shao, and H. Tang, "Numerical methods for nonlinear dirac equation," *Journal of Computational Physics* **245** (2013) 131–149.
https://www.sciencedirect.com/science/article/pii/S002199911300209X.

[36] F. Fillion-Gourdeau, E. Lorin, and A. D. Bandrauk, "Numerical solution of the time-dependent dirac equation in coordinate space without fermion-doubling," *Computer Physics Communications* **183** no. 7, (2012) 1403–1415.
https://www.sciencedirect.com/science/article/pii/S0010465512000653.

[37] E. Lorin and A. Bandrauk, "A simple and accurate mixed p0–q1 solver for the maxwell–dirac equations," *Nonlinear Analysis: Real World Applications* **12** no. 1, (2011) 190–202.
https://www.sciencedirect.com/science/article/pii/S1468121810001288.

[38] F. Fillion-Gourdeau, H. J. Herrmann, M. Mendoza, S. Palpacelli, and S. Succi, "Formal analogy between the dirac equation in its majorana form and the discrete-velocity version of the boltzmann kinetic equation," *Phys. Rev. Lett.* **111** (Oct, 2013) 160602.
https://link.aps.org/doi/10.1103/PhysRevLett.111.160602.

[39] F. m. c. Fillion-Gourdeau, S. MacLean, and R. Laflamme, "Algorithm for the solution of the dirac equation on digital quantum computers," *Phys. Rev. A* **95** (Apr, 2017) 042343. https://link.aps.org/doi/10.1103/PhysRevA.95.042343.

[40] A. M. Childs, Y. Su, M. C. Tran, N. Wiebe, and S. Zhu, "Theory of trotter error with commutator scaling," *Phys. Rev. X* **11** (Feb, 2021) 011020.
https://link.aps.org/doi/10.1103/PhysRevX.11.011020.

[41] X. Antoine, F. Fillion-Gourdeau, E. Lorin, and S. MacLean, "Pseudospectral computational methods for the time-dependent dirac equation in static curved spaces," *Journal of Computational Physics* **411** (Jun, 2020) 109412.
http://dx.doi.org/10.1016/j.jcp.2020.109412.

[42] A. M. Childs, "On the relationship between continuous- and discrete-time quantum walk," *Communications in Mathematical Physics* **294** no. 2, (Oct, 2009) 581–603.
https://doi.org/10.1007%2Fs00220-009-0930-1.

[43] A. M. Childs and J. Goldstone, "Spatial search and the dirac equation," *Phys. Rev. A* **70** (Oct, 2004) 042312. https://link.aps.org/doi/10.1103/PhysRevA.70.042312.

[44] G. H. Low and I. L. Chuang, "Hamiltonian Simulation by Qubitization," *Quantum* **3** (July, 2019) 163. https://doi.org/10.22331/q-2019-07-12-163.

[45] A. Gilyén, Y. Su, G. H. Low, and N. Wiebe, "Quantum singular value transformation and beyond: exponential improvements for quantum matrix arithmetics," in *Proceedings of the 51st Annual ACM SIGACT Symposium on Theory of Computing*. ACM, Jun, 2019. https://doi.org/10.1145%2F3313276.3316366.

[46] J. M. Martyn, Z. M. Rossi, A. K. Tan, and I. L. Chuang, "Grand unification of quantum algorithms," *PRX Quantum* **2** no. 4, (Dec, 2021) . https://doi.org/10.1103%2Fprxquantum.2.040203.

[47] A. M. Childs, "Universal computation by quantum walk," *Physical Review Letters* **102** no. 18, (May, 2009) . https://doi.org/10.1103%2Fphysrevlett.102.180501.

[48] A. M. Childs, D. Gosset, and Z. Webb, "Universal computation by multiparticle quantum walk," *Science* **339** no. 6121, (Feb, 2013) 791–794. https://doi.org/10.1126%2Fscience.1229957.

[49] J. Thomas, *Numerical Partial Differential Equations: Finite Difference Methods*. Texts in Applied Mathematics. Springer New York, 2013. https://books.google.co.jp/books?id=83v1BwAAQBAJ.

[50] G. Smith, G. Smith, and G. Smith, *Numerical Solution of Partial Differential Equations: Finite Difference Methods*. Oxford applied mathematics and computing science series. Clarendon Press, 1985. https://books.google.co.jp/books?id=hDpvljaHOrMC.

[51] D. Gottlieb and S. A. Orszag, *Numerical analysis of spectral methods: theory and applications*. SIAM, 1977.

[52] J. Boyd, *Chebyshev and Fourier Spectral Methods: Second Revised Edition*. Dover Books on Mathematics. Dover Publications, 2001. https://books.google.co.jp/books?id=i9UoAwAAQBAJ.

[53] C. Canuto, M. Hussaini, A. Quarteroni, and T. Zang, *Spectral Methods: Fundamentals in Single Domains*. Scientific Computation. Springer Berlin Heidelberg, 2007. https://books.google.co.jp/books?id=DFJB0kiq0CQC.

[54] F. Chatelin, *Spectral approximation of linear operators*. SIAM, 2011.

[55] M. Rieutord, B. Dubrulle, and P. Grandclément, "Introduction to spectral methods," *European Astronomical Society Publications Series* **21** (2006) 153–180.

[56] J. W. Cooley and J. W. Tukey, "An algorithm for the machine calculation of complex fourier series," *Mathematics of Computation* **19** (1965) 297–301.

[57] B. Fornberg, *A Practical Guide to Pseudospectral Methods*. Cambridge Monographs on Applied and Computational Mathematics. Cambridge University Press, 1998. https://books.google.co.jp/books?id=IqJoihDba3gC.

[58] P. W. Shor, "Polynomial-time algorithms for prime factorization and discrete logarithms on a quantum computer," *SIAM Review* **41** no. 2, (1999) 303–332. https://doi.org/10.1137/S0036144598347011.

[59] A. M. Childs, J.-P. Liu, and A. Ostrander, "High-precision quantum algorithms for partial differential equations," *Quantum* **5** (Nov., 2021) 574. https://doi.org/10.22331/q-2021-11-10-574.

[60] I. Kassal, S. P. Jordan, P. J. Love, M. Mohseni, and A. Aspuru-Guzik, "Polynomial-time quantum algorithm for the simulation of chemical dynamics," *Proceedings of the National Academy of Sciences* **105** no. 48, (2008) 18681–18686.

[61] Y. Su, D. W. Berry, N. Wiebe, N. Rubin, and R. Babbush, "Fault-tolerant quantum simulations of chemistry in first quantization," *PRX Quantum* **2** no. 4, (Nov, 2021) . https://doi.org/10.1103%2Fprxquantum.2.040332.

[62] F. M. Toyama and Y. Nogami, "Harmonic oscillators in relativistic quantum mechanics," *Phys. Rev. A* **59** (Feb, 1999) 1056–1062. https://link.aps.org/doi/10.1103/PhysRevA.59.1056.

[63] A. F. Shaw, P. Lougovski, J. R. Stryker, and N. Wiebe, "Quantum Algorithms for Simulating the Lattice Schwinger Model," *Quantum* **4** (Aug., 2020) 306. https://doi.org/10.22331/q-2020-08-10-306.

[64] X.-Q. Zhou, T. C. Ralph, P. Kalasuwan, M. Zhang, A. Peruzzo, B. P. Lanyon, and J. L. O'Brien, "Adding control to arbitrary unknown quantum operations," *Nature Communications* **2** no. 1, (Aug, 2011) 413. https://doi.org/10.1038/ncomms1392.

[65] P. J. Ollitrault, G. Mazzola, and I. Tavernelli, "Nonadiabatic molecular quantum dynamics with quantum computers," *Phys. Rev. Lett.* **125** (Dec, 2020) 260511. https://link.aps.org/doi/10.1103/PhysRevLett.125.260511.

[66] S. S. Bullock and I. L. Markov, "Asymptotically optimal circuits for arbitrary n-qubit diagonal comutations," *Quantum Info. Comput.* **4** no. 1, (Jan, 2004) 27–47.

[67] P. Krekora, Q. Su, and R. Grobe, "Klein paradox with spin-resolved electrons and positrons," *Phys. Rev. A* **72** (Dec, 2005) 064103. https://link.aps.org/doi/10.1103/PhysRevA.72.064103.

[68] C. Rovelli, *Quantum Gravity*. Cambridge Monographs on Mathematical Physics. Cambridge University Press, 2004. https://books.google.co.jp/books?id=HrAzTmXdssQC.

[69] N. V. Dang, "Renormalization of quantum field theory on curved space-times, a causal approach." 2013. https://arxiv.org/abs/1312.5674.

[70] D. Thouless, *The Quantum Mechanics of Many-Body Systems: Second Edition*. Dover Books on Physics. Dover Publications, 2014. https://books.google.co.jp/books?id=GaD6AQAAQBAJ.

[71] M. D. Pollock, "On the Dirac equation in curved space-time," *Acta Phys. Polon. B* **41** (2010) 1827–1846.

[72] K. Konno and M. Kasai, "General Relativistic Effects of Gravity in Quantum Mechanics: A Case of Ultra-Relativistic, Spin 1/2 Particles," *Progress of Theoretical Physics* **100** no. 6, (12, 1998) 1145–1157, https://academic.oup.com/ptp/article-pdf/100/6/1145/5268793/100-6-1145.pdf. https://doi.org/10.1143/PTP.100.1145.